

Learning Quantum Systems

Valentin Gebhart¹, Raffaele Santagati², Antonio Andrea Gentile³, Erik Gauger⁴, David Craig⁵, Natalia Ares⁶, Leonardo Banchi^{7,8}, Florian Marquardt⁹, Luca Pezze^{1,†}, and Cristian Bonato^{4,*}

¹QSTAR, INO-CNR and LENS, Largo Enrico Fermi 2, 50125 Firenze, Italy

²Boehringer Ingelheim, Quantum Lab, Doktor-Boehring-Gasse 5-11, 1120 Vienna, Austria

³Pasqal SAS, 7 Rue L. de Vinci, 91300, Massy, France

⁴School of Engineering and Physical Sciences, SUPA, Heriot-Watt University, Edinburgh, EH14 4AS, United Kingdom

⁵Department of Materials, University of Oxford, Oxford OX1 3PH, United Kingdom

⁶Department of Engineering Science, University of Oxford, Oxford OX1 3PJ, United Kingdom

⁷Department of Physics and Astronomy, University of Florence, via G. Sansone 1, I-50019 Sesto Fiorentino (FI), Italy

⁸INFN Sezione di Firenze, via G. Sansone 1, I-50019, Sesto Fiorentino (FI), Italy

⁹Max Planck Institute for the Science of Light and Friedrich-Alexander-Universität Erlangen-Nürnberg, Erlangen, Germany

†e-mail: luca.pezze@ino.cnr.it

*e-mail: c.bonato@hw.ac.uk

ABSTRACT

Quantum technologies hold the promise to revolutionise our society with ground-breaking applications in secure communication, high-performance computing and ultra-precise sensing. One of the main features in scaling up quantum technologies is that the complexity of quantum systems scales exponentially with their size. This poses severe challenges in the efficient calibration, benchmarking and validation of quantum states and their dynamical control. While the complete simulation of large-scale quantum systems may only be possible with a quantum computer, classical characterisation and optimisation methods – supported by cutting edge numerical techniques – can still play an important role.

Here, we review classical approaches to learning quantum systems, their correlation properties, their dynamics and their interaction with the environment. We discuss theoretical proposals and successful implementations in different physical platforms – such as spin qubits, trapped ions, photonic and atomic systems, and superconducting circuits. This review provides a brief background for key concepts recurring across many of these approaches – such as the Bayesian formalism or Neural Networks – and outlines open questions.

1 Introduction

Experiments exploring quantum physics have reached impressive levels in the control and the engineering of systems with increasing complexity and coherent degrees of freedom¹⁻³. The development of techniques for the characterisation of quantum states, their dynamics and possible measurement observables is motivated by ground-breaking applications in communication, computing, sensing and simulation. Yet, the exponential complexity of quantum systems poses significant challenges for their efficient description. This quest is currently stimulating a broad and interdisciplinary community to develop novel learning algorithms and techniques, with various levels of approximation. Learning quantum systems in a practical way is crucial for harnessing efficient techniques for quantum control and optimisation, broadly applicable to a variety of physical platforms such as spin qubit, trapped ions, photonic and atomic systems, as well as superconducting circuits. For instance, in the context of quantum computation, it is important to calibrate and benchmark quantum gates and operations implemented in the actual device, and to prepare qubit states with high fidelity. In quantum sensing, while learning quantum states and their dynamics is not strictly necessary, it is nevertheless crucial for the optimization of quantum state preparation, parameter encoding and measurement, with the target of improving the accuracy and precision of the device. Furthermore, tomographic methods can facilitate efforts in quantum simulations, to understand properties of ground and excited states in the systems and/or to categorise quantum phases of matter.

While the full simulation of large quantum systems may only be possible with a quantum computer⁴, classical methods for the characterisation of systems of medium size⁵ (e.g. of the order of hundreds of qubits) are currently playing a key role. Such

an approach is currently applied with great success in experiments, also shedding new light on fundamental properties such as entanglement, quantum superpositions and nonlocality.

Here, we provide a broad overview of a recently developed suite of different classical learning techniques that provide full or partial knowledge about the properties of quantum systems, including their interaction with the environment, as well as learning ways to better measure and control them. This review is structured in three main parts, related to learning quantum states, quantum dynamics and quantum measurements (see Fig. 1 for a schematic overview), including a final section devoted to applications of learning techniques for the optimisation of quantum experiments. We also provide a succinct background of the key concepts recurring across many of these approaches - such as the Bayesian formalism and [Neural Networks \(NNs\)](#) - and outline important open questions. Our overview of the literature targets a highly multidisciplinary audience, including quantum information physicists, statisticians, engineers and computer scientists, which characterizes the community involved in this field. While not covering technical details on the different learning methods, we make sure to provide pertinent references to the reader.

We do not discuss learning approaches based on quantum algorithms, including quantum machine learning, and we refer the reader to reviews on that subject⁶⁻⁸. Beyond that, there are many existing excellent reviews that cover and develop some other aspects related to our discussion, such as the use of machine learning techniques for quantum systems and for physics more generally⁸⁻¹¹, for the foundations of quantum theory¹² and computer-inspired design of quantum experiments¹³.

2 Learning Quantum States

The reconstruction of quantum states from experimental measurements is crucial for characterising the performance of near-term quantum hardware in terms of fidelity with target states, expectation values of local or nonlocal observables, correlation functions, and other properties. Accurately learning quantum states is also a key requirement for studying fundamental physics, such as the entanglement of the generated quantum states or the identification of quantum phases of matter. In the following, we first discuss the reconstruction of quantum states in a general setting, and then review a variety of assumptions that render this task more efficient. Finally, we discuss methods that address cases for which only particular properties of the quantum states are required, and conclude with an overview on optimal qubit readout.

2.1 Quantum state tomography

The process of inferring an unknown quantum state ρ from the measurement of multiple identically-prepared copies is known as [Quantum State Tomography \(QST\)](#)¹⁴⁻²¹. Here, we will focus on [QST](#) of finite-dimensional discrete-variable systems, such as multi-qubit systems. For tomographic methods in continuous-variable systems, including Wigner tomography to reconstruct the state of an optical mode, we refer to Refs.^{21,22}.

The most-widely used [QST](#) technique is based on **maximum-likelihood estimation**. This method searches for the quantum state featuring the largest probability, or likelihood, of the observed measurement results^{18,21-23}. Here, the likelihood of a series of m measurement results is given by

$$\mathcal{L}[\rho] = \prod_{j=1}^m \text{Tr}[\rho E_{\mu_j}], \quad (1)$$

where E_{μ_j} is one of the K elements of a [Positive-Operator Valued Measure \(POVM\)](#) (namely satisfying $E_{\mu} \geq 0$ and $\sum_{\mu=1}^K E_{\mu} = 1$) corresponding to the j th measurement result μ_j . The maximum-likelihood state, defined as $\rho = \arg \max_{\sigma} \mathcal{L}[\sigma]$, can be obtained by iterative algorithms, such as^{24,25}

$$\rho_{i+1} = \mathcal{N}_i R(\rho_i) \rho_i R(\rho_i), \quad (2)$$

where $R(\rho) = \sum_{j=1}^m E_{\mu_j} / \text{Tr}[\rho E_{\mu_j}]$, and \mathcal{N}_i is a normalisation constant. Alternatively, one can use **Bayesian approaches** (see Fig 2a, Box A), providing a natural way to include prior information and to compute error bars²⁶⁻²⁹ and confidence regions^{30,31} for the estimates (see Box A). In real-time [QST](#)^{28,32,33}, the observed data are analysed simultaneously to their recording, and thus **adaptive techniques** such as self-guided [QST](#)^{34,35} can be used to optimise the data acquisition procedure.

Generally, [QST](#) should search through the whole set of degrees of freedom of a quantum state, which scale exponentially with the number of qubits N . For larger N , this scaling results in inefficiencies of [QST](#) due to (i) the requirement of increasing amounts of measurement data³⁶, and (ii) the increasing complexity of classical post-processing³⁷. For instance, any tomographic method that can estimate an arbitrary state ρ up to an error ϵ in trace distance is shown to require $\mathcal{O}(4^N / \epsilon^2)$ measurements settings³⁶. These obstacles highlight the inefficiency of general [QST](#), already for the current generation of controllable quantum systems³⁸, and the need for new approaches to make [QST](#) practical.

2.2 Efficient quantum state tomography

Several approaches have been proposed to overcome the severe scaling of full QST. The techniques we discuss below show an improved scalability whenever the quantum state can be described by a specific ansatz, and enable QST of highly entangled quantum states of up to about a hundred of qubits, which is unfeasible for standard QST methods.

Compressed sensing^{37,39} can be applied to reconstruct a state of low-rank, i.e. whose density operator is described by a sparse matrix. Here, random Pauli measurements are used to reconstruct the unknown state via a convex optimisation algorithm. This method drastically reduces the number of measurements which, however, still scales exponentially with the number of qubits N . Compressed sensing can also be used to construct a low-rank estimate that approximates an unknown general state⁴⁰.

If the state is symmetric under permutations of the qubits, the number of tomographic measurements can be reduced to scale only quadratically with N by employing **permutationally-invariant QST**^{41,42}. This method can also be used to estimate the permutationally-invariant part of a general state. Similarly, for systems of identical particles, it is possible to exploit the symmetry of the state to significantly reduce the number of measurement settings^{43–46}. Examples include the reconstruction of a high-spin state⁴³, or the reconstruction of the state of many bosons in multiple modes⁴⁵. Moreover, the number of measurement settings can be reduced to one via the use of a polynomial number of ancillary systems^{45–48}.

A third method is the use of **tensor networks** to represent quantum states^{49–53}. Any pure quantum state can be written as a matrix product state

$$|\psi\rangle = \sum_{x_1, \dots, x_N} \text{Tr} \left[A_{x_1}^{[1]} A_{x_2}^{[2]} \dots A_{x_N}^{[N]} \right] |x_1 x_2 \dots x_N\rangle, \quad (3)$$

where $x_n \in \{0, 1\}$ labels the computational basis of the n th qubit, and $A_{x_n}^{[n]}$ are complex matrices of sufficient dimension⁴⁹. The maximal dimension of the $A_{x_n}^{[n]}$ is called bond dimension, and if it is small, the description of the state and its tomography are efficient, i.e. linear in N ⁵⁰. Even though matrix product states of low bond dimension cannot describe an arbitrary quantum state, they succeed to reconstruct the ground states of many common Hamiltonians.

Recently, NNs have been used to perform QST^{54–57}. In particular, a wide class of states can be modeled by a so-called **Restricted Boltzmann Machine (RBM)** (Box B and Fig. 3(b)), suitably adapted to the quantum setting^{54,58,59}. In this description, the parameters of the state are encoded into the weights of a NN that can be learned efficiently⁵⁴. The ansatz is given by $|\psi\rangle = \sum_{\mathbf{x}} \psi(\mathbf{x}) |\mathbf{x}\rangle$ where \mathbf{x} labels the computational basis vectors and, up to a normalisation factor, $\psi(\mathbf{x}) \propto \sqrt{p_a(\mathbf{x})} e^{i \log |p_\phi(\mathbf{x})|/2}$, where

$$p_k(\mathbf{x}) = \sum_{\mathbf{h}} e^{\sum_{ij} W_{ij}^k h_i x_j + \sum_j b_j^k x_j + \sum_i c_i^k h_i} \quad (4)$$

corresponds to a Gibbs distribution of a NN consisting of a visible layer (\mathbf{x}) and a hidden layer (\mathbf{h}), with weights $\{W_{ij}^k, b_j^k, c_i^k\}$ to encode the amplitudes ($k = a$) and the phases ($k = \phi$) of $|\psi\rangle$, and $\mathbf{h} = (h_1, \dots, h_w)$ where w is the number of neurons in the hidden layer. QST can also be interpreted as a generative adversarial game between two players (Box B and Fig. 3(c)), a generator trying to produce convincing approximations to the state and a discriminator trying to distinguish real states from generated ones⁶⁰. As such, classical and quantum **Generative Adversarial Networks (GANs)** have been employed for QST^{61,62}, with fewer measurements required when prior knowledge is available.

2.3 Extracting specific features of a quantum state

In cases when one is only interested in some specific properties of ρ , the intractability of full QST can be avoided by tailoring the measurement and post-processing to the specific property. Most prominently, several methods have been developed to efficiently measure entanglement properties^{63,64} such as entanglement entropies (e.g. using random measurements^{65,66}), metrologically-useful entanglement (e.g. Fisher information^{67,68} or spin-squeezing parameters⁶⁴), entanglement witnesses (i.e. measuring the fidelity to an entangled target state⁶⁹), and entanglement measures (e.g. the concurrence⁷⁰). Recently, NNs have been employed to measure the entanglement between two arbitrary subsystems⁷¹ and to identify single-mode nonclassicality⁷² without requiring full QST (Fig. 3(a)). NNs also offer promising routes for the identification of quantum phases of matter and quantum phase transitions^{73–79}, especially in disordered or topological phases, where no conventional order parameter exists.

If the measurements of the unknown state are randomly drawn from a fixed (but possibly unknown) distribution, the outcome probabilities of future measurements can be approximately learned (probably-approximately-correct, or PAC-learned) after merely a linear number of measurements^{80,81}. This insight has been strengthened in the recently introduced framework of **classical shadows**^{82,83} that can be used to efficiently estimate $\mathcal{O}(e^m)$ target functions $\text{Tr}[\rho O_i]$ from m measurements of ρ . Here, a series of random projective measurements from a fixed ensemble \mathcal{U} is performed. These measurements average to the quantum channel $\mathcal{M}[\rho] = |\mathcal{U}|^{-1} \sum_{U \in \mathcal{U}} \sum_{\mu_U} P_{\mu_U} \text{Tr}[\rho P_{\mu_U}]$, where U represents a measurement setting (namely, a unitary transformation applied before a measurement in the computational basis) with possible measurement outcomes μ_U , where

each outcome μ_U corresponds to the projector P_{μ_U} and is observed with probability $\text{Tr}[\rho P_{\mu_U}]$. For instance, an experimentally accessible measurement ensemble \mathcal{U} consists of tensor products of single-qubit Pauli measurements⁸². The classical shadow of ρ for the j th measurement is then defined as

$$\rho_s^{(j)} = \mathcal{M}^{-1}[P_{\mu_j}], \quad (5)$$

where P_{μ_j} is the projector of the j th measurement outcome μ_j . Note that since the map \mathcal{M}^{-1} is not a quantum channel, $\rho_s^{(j)}$ is not a valid quantum state. However, each classical shadow results in an estimate $\text{Tr}[\rho_s^{(j)} O_i]$ of the i th target function. After a statistical inference step (median-of-means), one obtains the final estimates of the target functions. In this way, the estimation of $\mathcal{O}(e^m)$ target functions $\text{Tr}[\rho O_i]$ requires only m random measurements⁸², where the proportionality factors depend on the choice of the measurement ensemble \mathcal{U} and the characteristics of the observables O_i . Note that the formalism can also be used to estimate nonlinear functions such as $\text{Tr}[\rho \otimes \rho O]$ ⁸². Classical shadows offer an advantage with respect to maximum-likelihood and Bayesian techniques in certain tasks described in Ref.⁸⁴. Finally, if the target functions only include Pauli observables, the formalism can further be derandomised to optimise its performance⁸⁵. Examples for applications of classical shadows are the efficient measurement of the entanglement entropy⁶⁶, or the estimation of the quantum Fisher information⁸⁶.

2.4 Optimising qubit readout

Performing **QST** is greatly facilitated by the availability of high-fidelity single-shot readout for each qubit state. A single-shot measurement typically consists of a time-resolved signal which is processed to produce histograms relating to the qubit being prepared in the ground or excited state, and a threshold of the readout value is chosen to resolve the two states^{87–90}.

Stochastic relaxation of the excited state causes an asymmetry in readout histograms that decreases readout fidelity by threshold classification. Clustering methods have been used to identify and discard such relaxation signals and increase fidelity in superconducting qubits⁹¹. However, while still increasing overall fidelity, similar methods have produced outlier results of lower quality than thresholding repetitive readouts⁹². Non-linear Bayesian filters have improved on threshold fidelities by considering the full time-resolved readout signal while accounting for relaxation⁹³ and stochastic turn-on times in spin-to-charge conversion readout⁹⁴. **NNs** have improved on threshold methods in diamond NV centres, which lack single-shot readout at room temperature⁹², and **NN** classifiers trained on synthetic time-resolved data have surpassed the performance of Bayesian filters in quantum-dot spin qubit readout⁹⁵. Multi-qubit states have been classified using **NNs** in trapped-ion qubits, where time-binned multi-channel data has provided the highest fidelity⁹⁶. **Recurrent Neural Networks (RNNs)** have been used to predict time-evolving qubit states from experimental noisy measurement traces⁹⁷.

While the availability of single-shot readout and projective quantum measurements facilitates learning of quantum systems, it is not necessarily a prerequisite and averaged readout can be used, in combination for example with Bayesian inference⁹⁸.

3 Learning quantum dynamics

The reconstruction of quantum evolution is important for establishing, for instance, channel fidelity in quantum communication, gate fidelity in quantum computing and optimal parameter encoding for sensing applications. Following the discussion of **QST**, we will first review assumption-free methods, and then move to methods that introduce specific dynamical models to simplify the characterisation. We will then discuss applications to quantum sensing and imaging.

3.1 Learning dynamics with Quantum Process Tomography

The task of fully reconstructing the dynamics of a quantum system driven by an underlying, unknown process is called **Quantum Process Tomography (QPT)**^{99,100}. In a typical setting, **QPT** results in the estimation of a given quantum process, by applying the latter to a set of fiduciary quantum states. The resulting output states are reconstructed via **QST**, allowing one to identify how the initial states evolved under the process. More formally, one can reconstruct the quantum channel Λ that describes the quantum process according to $\rho_{\text{out},i} = \Lambda[\rho_{\text{in},i}]$, where $\{\rho_{\text{in},i}\}_i$ is an arbitrary set of input states, and each $\rho_{\text{in},i}$ is associated to a corresponding output state $\rho_{\text{out},i}$ ^{101–103}.

In the same way as **QST**, **QPT** requires a number of measurements and classical post-processing that scale exponentially with the size of the quantum system under study¹⁰⁴. Such punishing scaling afflicts, for example, methods based on **maximum likelihood inference**¹⁰⁵, which additionally show a high sensitivity to errors in initial states, gates and measurements¹⁰⁶.

Different methods have been explored to overcome these limitations. An example is **randomised benchmarking**¹⁰⁷ which estimates the error rate (or fidelity) of a quantum process from a sequence of random repetitions of the process^{108–111}. However, randomised benchmarking does not reconstruct the process matrix Λ and thus does not deliver a fully general characterisation of the quantum process. For processes Λ that can be represented as a sparse superoperator, **compressed sensing (CS)** methods can be employed to reduce reconstruction costs^{109,112,113}, cf. Sec. 2.2.

Alternative approaches exploit more sophisticated methodologies. For example, building on methods introduced for QST (see Sec. 2.2), tensor networks can lead to drastically reduced resource requirements^{114–116}. GAN-based approximations of the superoperator Λ have also been proposed as an efficient method for QPT⁶². Other methods exploit NNs to generalise QPT to the characterisation of time dependent spin systems¹¹⁷, while yet another class reconstructs a unitary quantum process by inverting the dynamics using a variational algorithm^{118,119}. RNNs have recently been shown to be useful in learning the non-equilibrium dynamics of a many-body quantum system from its nonlinear response under random driving¹²⁰.

3.2 Reconstructing the generators of Hamiltonian quantum dynamics

Reconstructing the general superoperator Λ is resource-demanding and one might not have access to the full set of observables required for full QPT. A commonly-used approach is the reconstruction of a specific dynamical model described by **generators**, e.g. a Hamiltonian model for a unitary evolution with a small number of tunable control parameters. These approaches leverage prior information about the system to simplify the reconstruction.

A first class of methods relies on the measurement of time traces of measurable observables^{121–123}. Hamiltonian parameters for a few qubits can be retrieved by fitting these time traces or by using **Fourier methods**. More sophisticated approaches rely on using **linear systems theory**, such as the eigenstate realisation algorithm^{124,125}. Here, after decomposing the Hamiltonian into Hermitian operators, the evolution can be described by a linear differential equation. The algorithm then follows linear systems theory, by adopting a *system realisation* from experimental data attained at regular time intervals, leading to a transfer function mapping input states to observables, from which one obtains the unknown parameters. More recent versions further refine these methods by extracting the eigenfrequencies of H from a complex time domain measurement and then recovering the eigenvectors of the Hamiltonian via constrained manifold optimisation¹²⁶.

A second class of methods employs (approximate) **Bayesian inference** (see Fig 2b). Computationally efficient Bayesian tomography, for example, has been used to characterise logic gates for spin qubits in silicon¹²⁷. A generation of Bayesian methods known as **Quantum Hamiltonian Learning (QHL)** infers a set of unknown parameters \mathbf{x} for a specific parametrisation $H(\mathbf{x}, \boldsymbol{\tau})$ ^{128–130}. Here, $\boldsymbol{\tau}$ represents a set of tunable control parameters that typically is just the evolution time t . It is assumed that the specific parametrisation $H(\mathbf{x}, \boldsymbol{\tau})$ offers a much more efficient reconstruction, as the number of parameters \mathbf{x} is usually much smaller than the number of parameters necessary to describe the most general Λ or H . The implementation of QHL requires estimating the likelihood $P(\mu|\mathbf{x}, \boldsymbol{\tau})$ for each of the discrete outcomes μ of a projective measurement, and using Bayes rule to update the belief on \mathbf{x} , encoded in the posterior distribution (see Box A). To extract $P(\mu|\mathbf{x}, \boldsymbol{\tau})$, QHL invokes access to a trusted simulator that can implement a controlled evolution by $H(\mathbf{x}, \boldsymbol{\tau})$ for different combinations of $(\mathbf{x}, \boldsymbol{\tau})$, prepare fiducial initial states, and perform projective measurements on the evolved states.

For few-qubit systems^{29,128,131}, the likelihood may be evaluated on a classical computer for all necessary combinations of $(\mathbf{x}, \boldsymbol{\tau})$. This becomes rapidly unfeasible for larger quantum systems and the quantum nature of the simulator becomes crucial^{129,130,132}. QHL has been successfully demonstrated in different experimental platforms, for various tasks, such as characterising NV centres in diamond^{133–135} or quantum sensing of magnetic fields^{136–138}, and can potentially be adapted for quantum control¹³⁹. QHL is more robust than e.g. Fourier analysis^{137,140} due to its Bayesian nature and the use of an adaptive choice of measurement settings according to the cumulative knowledge inferred about the system.

One of the main drawbacks of QHL is that it requires the knowledge of the parametrisation $H(\mathbf{x})$. Recently, this limitation has been addressed by the use of **Quantum Model Learning Agents (QMLAs)**^{135,141} (Fig 2c), where the artificial agent constructs different candidate Hamiltonian models $H_i(\mathbf{x})$ starting from a number of simple, generic terms h_v (e.g. Pauli matrices). The latter are selected and combined via tree searches or genetic algorithms to generate new candidate models. After a parameter training via QHL, the different $H_i(\mathbf{x})$ are systematically compared against remaining candidates by metrics \mathcal{B} such as Bayes factors or modified Elo-ratings^{135,141}, and the least performing instances are discarded (see Fig. 2c).

The task of Hamiltonian learning has also been addressed by **deep learning methods**. For example, NNs were used to recover Hamiltonians from local measurements of ground states¹⁴², and RNNs can learn time-dependent target Hamiltonians from time traces of single-qubit measurements without knowledge of the ground states¹⁴³. However, the training of NNs is notoriously time-consuming. A possibility to circumvent this problem is to include inductive bias coming from the known physical laws describing the system. One option consists of Neural Ordinary Differential Equations (**Neural Ordinary Differential Equations (NODEs)**) that include the system's differential equations¹⁴⁴ or the system's Lagrangian function¹⁴⁵ in the structure of the NN, see Fig. 3(d). NODEs have been applied to the optimal control of a qubit that is modeled as a closed system¹⁴⁶ and as a monitored (and thus stochastic) system¹⁴⁷. A second example are Physics-Inspired Neural Networks (**Physics-Informed Neural Networks (PINNs)**) which directly model the solution of the system's differential equations by including the latter in the cost function¹⁴⁸, see Box B. Several software suites readily adaptable or devoted specifically to PINNs have been developed both in research and industrial environments^{149–152}. Similar to the QHL methods above, the availability of the system's dynamical equations crucially reduces the complexity of the training whilst preserving excellent performance. Recent improvements extend PINNs to the optimisation of several competing PINN models^{153,154}, and classical

PINNs may be supported by QNNs, i.e., by employing parameterised quantum circuits^{155,156}. These circuits would then act as a quantum simulator, possibly surpassing limitations in the expressivity of classical NNs of feasible size^{157,158}. To this date, the application of PINNs to quantum systems is in its very infancy, with early applications exploring simple instances of the Schrödinger equation^{148,159} and the possibility to control dynamically-corrected quantum gates¹⁶⁰. A final example are 'gray-box' approaches^{161,162} that combine a NN as a 'black box' to learn the Hamiltonian with a physically-understandable 'white box' embedding the rules of quantum mechanics, such as state evolution. This approach is able to address the uncertainty in the Hamiltonian model, distortions caused by undesired macroscopic dynamics and imperfect measurements.

If the target Hamiltonian H is local and one is provided with **knowledge of a single (approximate) eigenstate** of H , it was shown that H can be reconstructed using resources that scale polynomially with the number of qubits^{163–165}. The technique consists of manipulating a covariance matrix of expectation values of Hermitian operators that span the space of local Hamiltonians. This approach can be extended to generic mixed states commuting with H ¹⁶⁶, and to situations where only local measurements of limited regions of the full systems are available¹⁶⁷. These methods, however, are still sensitive to noise^{163,166}.

3.3 Reconstructing open quantum system dynamics

When the dynamics of a quantum system of interest is not sufficiently isolated from its environment, the Hamiltonian description fails and the system has to be treated as an **open quantum system**^{168,169}. For a memory-less environment, the system's dynamics is Markovian and the evolution of the quantum state ρ can be described by the Gorini, Kossakowski, Sudarshan and Lindblad (GKS-L) master equation^{170,171}

$$\dot{\rho} = -i[H, \rho] + \sum_j \left(L_j \rho L_j^\dagger - \{L_j^\dagger L_j, \rho\} / 2 \right), \quad (6)$$

where $\{A, B\} = AB + BA$, H is the Hamiltonian, and L_k are the Lindblad operators that describe the dissipative process. The reconstruction of H and L_k from measurement data has been dubbed **Lindblad tomography**¹⁷², where an algorithm based on maximum likelihood estimators was presented. Alternatively, the generators can be reconstructed from the measurement of time traces and linear system realisation theory¹⁷³. Local Markovian dynamics can also be recovered via local measurements when steady states can be prepared¹⁷⁴, adopting techniques similar to those outlined for Hamiltonian reconstruction, when knowledge of approximate eigenstates is available.

Whilst often providing an excellent description of the quantum dynamics, the assumptions resulting in a Markovian evolution are not fulfilled in general^{168,175,176}. In non-Markovian dynamics, the state at time $t + dt$, ρ_{t+dt} , depends not only on ρ_t but also on the system's history at earlier times. This evolution can be expressed by the master equation¹⁶⁸ $\dot{\rho}_t = \int_0^t ds \mathcal{K}(t, s) \rho_s$ with a time-nonlocal superoperator \mathcal{K} . Alternatively, we can employ a process tensor formalism¹⁷⁷, where the time-discretised unitary evolution operator of the system is interleaved with environmental influence interventions from a 'quantum-comb'-like process tensor. Whilst the dimension of this process tensor scales exponentially with the number of time steps, often, e.g. when memory effects are short-range, it is possible to express the process tensor in compressed matrix operator form (c.f. Eq. (3)), which can be efficiently constructed from knowledge of the underlying microscopic model^{178,179} or reconstructed from time measurements^{177,180}. Such **process tensor tomography** generalises QPT, thereby providing access to multi-time correlations, and it has recently been shown to be compatible with NISQ devices¹⁸¹. Alternatively, methods based on NNs can be employed to reconstruct non-Markovian quantum dynamics^{182,183}. Generally, these approaches entail reduced physical insight, however, in some cases a degree of interpretability can be preserved, e.g., by rendering a GKS-L master equation (6) non-Markovian through effective time-dependent Lindblad operators that depend on the entire history. In one such example, the matrix elements of L_k were expressed using RNNs¹⁸², i.e. neural networks of a type that are routinely applied to model long-range memory effects.

3.4 Parameter estimation with quantum sensors

Quantum sensors^{64,184,185} are devices used to estimate parameters – such as magnetic fields, external forces, accelerations, etc. – that modify (e.g. via a dynamical parameter encoding) a quantum state. Quantum systems provide a key advantage in terms of their small size (resulting in high spatial resolution). Furthermore, quantum effects such as coherence, squeezing and entanglement can increase the sensitivity of the device^{64,185}. The optimal uncertainty for the unbiased estimation of a parameter θ , based on m measurement results, can be quantified by the quantum Cramer-Rao bound^{186,187}

$$(\Delta\theta)^2 = \frac{1}{mF_Q(\theta)}, \quad (7)$$

where F_Q is the **Quantum Fisher Information (QFI)**, depending on the sensor's output state ρ_θ . Equation (7) is understood as the sensitivity achievable with an optimal estimator and using optimal measurement observables¹⁸⁷. In a Bayesian setting (see Box A), Eq. (7) provides the asymptotic posterior variance using optimal measurements. It is important to emphasise that the

frequentist Cramer-Rao bound Eq. (7) does not hold for Bayesian inference and, thus, Bayesian bounds must be used instead¹⁸⁸. Recently, it has been shown that NNs can then be trained to construct estimators^{189–191} or Bayesian posterior distributions¹⁹² based on supervised learning techniques and using limited calibration data. In both cases, a well-calibrated network can be used for post-processing data that saturate Eq. (7) for a sufficiently large number of measurements. These NN-based estimation methods are valuable when one is lacking simple models for the output probability distribution of the sensor, e.g. when the number of possible measurement events is large.

A notable result in quantum sensing is the relation between uncertainty and entanglement^{64,193}: separable states of N qubits that undergo a collective spin rotation (as common in many applications) can achieve, at best⁶⁷, a QFI $F_Q = N$. Entanglement is necessary⁶⁷ for $F_Q > N$, while genuine multipartite entanglement is necessary^{194,195} to achieve the ultimate limit $F_Q = N^2$. Interestingly, multipartite entanglement witnessed by the QFI^{194,195} is found in a variety of many-body phenomena such as quantum phase transitions, quantum chaos, quenches, random states, and so on.

In the case of the joint estimation of d parameters $\theta_1, \dots, \theta_d$, the $d \times d$ covariance matrix of estimators is bounded the inverse (when it exists) of the QFI matrix^{186,196}. In general, when estimating multiple parameters, there is no optimal observable with which the quantum Cramer-Rao bound can be saturated. This problem is due to non-commutativity of the different parameter encoding transformations^{186,196} and the more involved Holevo-Cramer-Rao bound must be used instead¹⁹⁷. For commuting encoding transformations, the interplay between mode and particle entanglement and the QFI matrix has been discussed in Ref.¹⁹⁸ and experimentally investigated with optical qubits¹⁹⁹.

3.5 Quantum Imaging, Target Detection and Pattern Recognition

As in quantum sensing, quantum-enhanced detection schemes use a combination of entangled states of light and carefully designed measurements to beat the classical limits. However, unlike metrological applications where the task is typically to estimate a continuous parameter, here the main task is to estimate a discrete variable, such as the binary variable describing the presence or absence of a target or the pixel values in the images. Because of the discrete nature of the problem, a quantum advantage cannot be quantified via the quantum Cramer-Rao bound Eq. (7), and alternative strategies have been proposed. A common approach is to first define a problem-dependent cost function and then compare the performance of entangled sensors with strategies based on coherent states only.

Since the field is vast, here we limit ourselves to NN-inspired methods and refer to existing reviews^{200,201} for a more extensive treatment. Entangled sensors have been used to define a quantum support vector machine able to more accurately classify the presence of a target²⁰². Moreover, entangled probes can be used to read binary images with enhanced precision and perform more accurate image classification²⁰³. While for full imaging each pixel must be accurately reconstructed, for pattern recognition errors are tolerated and less precise detectors are allowed. This intuitive idea was formalised in²⁰³ by showing that the error with optimal detectors decreases exponentially with the number of bits that must be flipped to switch class. Finally, quantum imaging can be enhanced by deep learning techniques^{204–206}, in order to increase the fidelity, discover deeper structure in data and overcome errors due to shot noise and background noise.

4 Learning quantum measurements

The characterisation of detectors is commonly given in terms of quantum efficiency, linearity, rate of dark counts, and spectral and temporal response. However, these aspects represent only an approximation of the actual operation of a detector and can introduce systematic errors that may strongly affect high-precision measurements or investigations of quantum effects. **Quantum Detection Tomography (QDT)**^{207,208} aims at reconstructing quantum measurement devices without any prior information or approximations. This characterization plays a key role in any quantum architecture.

Realistic (noisy) detectors are non-projective and thus QDT consists in the tomographic reconstruction of a set of POVM operators E_μ ^{207–209}. These operators describe the probability of a generic measurement detection event μ according to the Born rule

$$\Pr(\mu) = \text{Tr}[\rho E_\mu], \quad (8)$$

given a probe state ρ . The standard QDT approach consists of inverting Eq. (8) using the experimentally-sampled probability distribution and for a suitably chosen set of probe states that must be tomographically complete, i.e., span the Hilbert subspace where the POVM elements are defined. As a simple example, we can consider an ideal (von Neumann) projective measurement $\Pr_{\text{id}}(\nu) = \langle \nu | \rho | \nu \rangle$, where $\{|\nu\rangle\}$ is a set of orthogonal states, and model a noisy detection by a Markov mapping $V \geq 0$ such that $\Pr_V(\mu) = \sum_\nu V_{\mu\nu} \Pr_{\text{id}}(\nu)$ is the probability of a detection event, depending on the specific choice of V . As $V_{\mu\nu}$ describes the probability to observe the result μ when ν should be ideally observed, it includes the detector's imperfections, and satisfies the normalization condition $\sum_\mu V_{\mu\nu} = 1$ for all ν . In this case, given the observed probabilities $\Pr(\mu)$, QDT corresponds to finding the matrix V that minimises the distinguishability between the probability distributions $\Pr(\mu)$ and $\Pr_V(\mu)$ (e.g. quantified by

the Kullback-Leibler divergence or the fidelity). Such an optimisation can be obtained via gradient descent or a maximum likelihood method. The corresponding POVM in Eq. (8) reads $E_\mu = \sum_v V_{\mu v} |v\rangle\langle v|$.

Different detector-tomography techniques have been developed and used experimentally, with a main application being the characterisation of optical photocounting^{210–212} and homodyne^{213,214} detection, and, more recently, qubit readout in quantum computing machines²¹⁵. With superconducting single photon detectors, QDT has provided a valuable tool to discriminate among different models to explain the basic physics underpinning the detection mechanism²¹⁶. Usual QDT methods require the precise calibration of probe states that, in turn, demands the precise knowledge of the measurement device, thus possibly inducing systematic errors^{217,218}. Self-characterising QDT techniques that do not rely on precisely-calibrated probe states have been demonstrated for single optical qubits²¹⁹.

5 Optimising quantum experiments

In this section, we briefly review a few selected applications of classical learning for the optimisation of quantum experiments.

5.1 Adaptive methods for quantum sensing

Quantum sensor can be optimized by harnessing **adaptive protocols**: these, that compute the optimal experimental settings from the current knowledge about the unknown parameter being estimated, following data acquisition. Indeed, while the optimal setting of the sensor depends, in general, on the unknown parameter being estimated, adaptive strategies can converge, asymptotically in the number of measurements, to the optimal configuration. Bayesian methods (see Box A) are well suited for adaptive optimisation^{220,221} (Fig 4a and b). Several adaptive protocols have focused on the optimisation of measurements^{220,222}, including numerical techniques such as particle swarm²²³ and differential evolution algorithms²²⁴. Recently, **Reinforcement Learning (RL)** has been employed to discover the whole sequence of optimal adaptive measurements of a qubit in the Bayesian framework²²¹. The optimization of probe states, e.g. in order to extend the bandwidth of entanglement-enhanced sensitivity, has been considered using analytical methods^{225,226} as well as variational^{227,228} and NN strategies²²⁹. Besides the optimisation of measurements and probe states, another possibility is to modify parameter encoding by adding control Hamiltonians^{230,231}, optimised efficiently via RL.

Experimentally, adaptive techniques have been employed, for example, to improve the sensitivity of optical phase sensing realizing a phase estimation protocol²²⁰, or in quantum sensors based on the single spin associated with the nitrogen-vacancy (NV) centre in diamond, a system widely used for nanoscale magnetic mapping and magnetic resonance^{137,138,232–235}. Due to the time constraints, a key consideration for online sensing is the cost of the processing procedure: simplified near-optimal methods might perform better than optimal but computationally-intensive ones. This is especially important in the tracking of time dependent magnetic fields in DC magnetometry^{136,137,236}.

5.2 Optimal control over the environment

Reconstructing the dynamics of a quantum system presents opportunities to establish a degree of control over the environment, for example with the goal of reducing the decoherence of the system. QHL has been used to suppress decoherence for a single spin qubit by a real-time compensation of nuclear-spin bath fluctuations²³⁷ and classical noise²³⁸. If the environment can be described by a quantum system, the learning process itself can be considered a control tool because the back-action of a quantum measurement perturbs the quantum state, for example by projecting the system to an eigenstate of the measurement²³⁹. Even though the random measurement outcomes result in random quantum states of the system, feedback can be used to make the control system deterministic²⁴⁰. Protocols have been suggested to extend a qubit's coherence by sequential Hamiltonian learning with real-time feedback from the measurement outcomes²⁴¹.

A similar idea is at the basis of quantum error correction, which is a general approach to counteract noise in quantum computation and quantum communication²⁴². More formally, given a general noisy evolution Λ , quantum error correction consists in finding a recovery channel \mathcal{R} such that

$$\mathcal{R}[\Lambda[\rho_S]] = \rho_S, \tag{9}$$

where ρ_S is defined in a subspace \mathcal{H}_S of the total Hilbert space. For applications in quantum sensing^{243–247}, it is further required that the recovery operation \mathcal{R} is such that $\mathcal{R}[\Lambda[\rho_S(\theta)]]$ follows a noiseless parameter-encoding dynamics in the subspace \mathcal{H}_S including quantum states with finite (possibly large) quantum Fisher information.

5.3 Optimal control of a quantum system

Other applications of **Machine Learning (ML)** methods to quantum technologies include the design of quantum gates^{248,249} or the identification and design of circuits for quantum error correction²⁵⁰. In particular, model-free RL is a powerful general approach to learn control strategies, where an agent (often implemented via a NN) observes and controls an "environment",

which might be a quantum device (see Fig.4c). The dynamics of the environment need not be known in advance: the agent will implicitly learn an approximate model while trying to find a good feedback control strategy. Overall, the agent tries to optimise a reward (e.g. defined in terms of final state fidelity for the case of state preparation). In so-called policy gradient approaches, this is done by implementing a parametrised stochastic policy $\pi_\theta(a|s)$ – the probability of an action a given an observed state s – and changing by gradient ascent the probabilities in any action sequence to maximise the average cumulative reward (see e.g. Ref¹⁰ for more details).

In theoretical studies, RL has been shown to discover feedback strategies for quantum error correction²⁵¹, obtain qubit control pulses for state preparation^{252,253}, and solve many other tasks (see Fig.4d and e). It is beginning to be implemented on experimental platforms, e.g. for superconducting qubit gate synthesis²⁵⁴ and also for adaptive characterisation of quantum systems²⁵⁵. A particular challenge consists in extracting the reward reliably from available experimental measurements and to make sure that the agent can be trained in a truly model-free way without any assumptions²⁵⁶.

5.4 Optimal design of experimental quantum setups

In addition to optimising control strategies for given experimental setups, one can also pursue the goal of optimising the setup itself. This may involve varying the components and how they are connected within the setup. In a quantum-optical setup, these might be linear and nonlinear components. Whole setups in this domain have been automatically discovered, optimising some desired property like the entanglement of multi-photon states produced at the output^{13,257}. It has then been possible to extract motifs from the generated setups and identify them as useful building blocks that implement some novel ideas: see Ref.¹³ for an overview of experimental implementations of optimised setup designs

6 Discussion and Perspectives

The application of classical algorithms and methods to quantum technologies offers possibilities to circumvent some of the obstacles in characterisation, calibration and validation posed by the exponential complexity of quantum systems and the intrinsic probabilistic nature of quantum measurements. In this review, we have focused on classical data-processing of measurement outcomes of quantum experiments and their optimisation towards a variety of tasks, ranging from learning states to controlling experimental setups. The fast progress of this field relies on the possibility to directly adapt efficient numerical methods already developed in computer science and statistics to solve demanding problems in quantum physics, such as the characterisation of quantum states, the identification of quantum phases of matter and entanglement witnesses, the reconstruction of quantum dynamics, the optimisation of parameters and operations, etc.

Most adaptive experiments to date have been harnessing Bayesian methods, due to their simple practical implementation. Bayesian inference, however, relies on the availability of explicit fitting models, precisely calibrated to the specific experimental setting. When such models are not available, or to remove the requirement of tedious calibration, neural networks can provide a better option, because of their superior expressivity. We expect that in the future, a growing number of experimental implementations will employ neural networks to model "black-box" quantum sensors or systems. This also holds for online parameter optimisation in adaptive experiments: while most experiments so far have relied on near-optimal simple analytical heuristics, deep RL has been suggested²²¹ as a "system-agnostic" procedure to generate optimised ready-to-use heuristics. We expect that NN-based inference and RL will be increasingly adopted by experiments, removing the need for manual derivation of experimental-design heuristics.

More generally, RL is a very promising approach in discovering from scratch feedback-control strategies for quantum devices, for goals ranging from state and device characterisation to error correction. While it works successfully for some tasks in simulations and also in first experiments, there are still multiple demanding challenges to be solved in this domain. Among them the need for the network agent to find simultaneously both a good control strategy and an interpretation of the noisy measurement data, the technical hurdles in experimentally implementing real-time feedback using neural networks, and the construction of good reward functions that help guide the optimisation while being accessible from experimental data.

Further opportunities come from developments of quantum computing hardware. While a classical computer processes the classical outcomes of quantum measurements, a quantum computer can directly handle "raw" quantum states from an experiment. The main advantage of this approach is that a quantum computer can perform joint measurements on several qubits, exploiting quantum entanglement. A recent paper²⁵⁸ showed that joint quantum measurements lead to substantial advantages for learning quantum systems, as they outperform single measurements in distinguishing quantum states even when the states are uncorrelated. A challenge for learning quantum states with a quantum processor is the need for a quantum-coherent interface between the quantum system under study and the quantum processor. This will require further research in "hybrid" quantum structures, where quantum sensors, devices and systems are interfaced to a quantum computer preserving quantum coherence.

The fact that advantages in learning quantum systems can already be demonstrated by current noisy intermediate quantum devices opens up exciting possibilities, that will become more and more important as we advance towards full fault-tolerant quantum computing.

Acknowledgements

The authors thank Chris Ferrie for useful discussions. CB is supported by the Engineering and Physical Sciences Research Council (EP/S000550/1 and EP/V053779/1), the Leverhulme Trust (RPG-2019-388) and the European Commission (QuantELCO, grant agreement No 862721). NA acknowledges support by the Royal Society (URF/R1/191150), EPSRC Platform Grant (EP/R029229/1), the European Research Council (grant agreement 948932) and FQXi Grant Number FQXI-IAF19-01. LB's work is supported by the U.S. Department of Energy, Office of Science, National Quantum Information Science Research Centers, Superconducting Quantum Materials and Systems Center (SQMS) under the contract No. DE-AC02-07CH11359, and by the INFN via the Qubit, SFT and INFN-ML projects. VG and LP acknowledge financial support from the European Union's Horizon 2020 research and innovation programme—Qombs Project, FET Flagship on Quantum Technologies Grant No. 820419.

Box A: Bayesian inference

Bayesian inference is a central method in statistical analysis that prescribes how to update a degree of belief about a hypothesis (e.g. that a set of unknown parameters $\boldsymbol{\theta} = \{\theta_1, \dots, \theta_d\}$ has the specific values $\boldsymbol{\phi} = \{\phi_1, \dots, \phi_d\}$) if new observations or evidence (e.g. a sequence of measurement results $\boldsymbol{\mu} = \{\mu_1, \dots, \mu_m\}$) are obtained. It is based on **Bayes' theorem**, which for parameter estimation takes the form

$$P(\boldsymbol{\phi}|\boldsymbol{\mu};\mathcal{C}) = \frac{P(\boldsymbol{\mu}|\boldsymbol{\phi};\mathcal{C})P(\boldsymbol{\phi})}{P(\boldsymbol{\mu};\mathcal{C})}, \quad (10)$$

dictating how to obtain the **posterior probability** $P(\boldsymbol{\phi}|\boldsymbol{\mu};\mathcal{C})$ from the **prior distribution** $P(\boldsymbol{\phi})$, using the likelihood $P(\boldsymbol{\mu}|\boldsymbol{\phi};\mathcal{C})$ of observing $\boldsymbol{\mu}$ with measurement settings \mathcal{C} if the true phase was $\boldsymbol{\phi}$, and a marginal probability $P(\boldsymbol{\mu};\mathcal{C})$ for normalisation. In quantum systems, $P(\boldsymbol{\mu}|\boldsymbol{\phi};\mathcal{C})$ is computed using Born's rule. Estimates and corresponding uncertainties (or confidence intervals) can be obtained directly from the Bayesian posterior: this provides a crucial advantage with respect to the frequentist approach that obtain parameter uncertainties from measurement histograms. If the measurement results $\boldsymbol{\mu}$ are independent, Bayes' theorem can be also written recursively in the form of a **Bayesian update** when observing the measurement result μ_j , see Fig. 2. The Laplace-Bernstein-von Mises theorem guarantees that, asymptotically in the number of measurements m and under mild regularity conditions (such as continuity, regular derivatives and absence of periodicity), the Bayesian posterior converges to a normal distribution

$$P(\boldsymbol{\phi}|\boldsymbol{\mu}) \rightarrow \sqrt{\frac{m \det F(\boldsymbol{\theta})}{2\pi}} e^{-\frac{m}{2}(\boldsymbol{\phi}-\boldsymbol{\theta})^T \cdot F(\boldsymbol{\theta}) \cdot (\boldsymbol{\phi}-\boldsymbol{\theta})}, \quad (11)$$

centred at $\boldsymbol{\theta}$ with a covariance given by the inverse of the Fisher Information matrix $F(\boldsymbol{\theta})$ with entries $[F(\boldsymbol{\theta})]_{ij} = \sum_{\boldsymbol{\mu}} P(\boldsymbol{\mu}|\boldsymbol{\theta}) \partial_{\theta_i} \log P(\boldsymbol{\mu}|\boldsymbol{\theta}) \partial_{\theta_j} \log P(\boldsymbol{\mu}|\boldsymbol{\theta})$, for a fixed measurement configuration.

A further advantage of Bayesian inference is that it allows a natural integration of **optimisation techniques**^{220,222,259,260}. At each point in time, the current knowledge $P(\boldsymbol{\phi}|\boldsymbol{\mu};\mathcal{C})$ about the parameters can be used to choose optimal experimental settings \mathcal{C} for the next measurement. In cases where the optimal measurement settings depend on the (unknown) parameters $\boldsymbol{\theta}$, adaptive techniques can significantly improve the performance and the requirements of the estimation protocol. A practical difficulty is that post-processing the Bayesian distribution requires to evaluate it on a grid of $\boldsymbol{\phi}$ values, which can be problematic for broad distributions and in multiparameter scenarios. An efficient Bayesian inference for the estimation of multiple parameters^{27,260,261} thus requires using approximate methods, such as particle-filtering and Sequential Monte Carlo methods^{128,259,262}, or structured filtering²⁶³ when dealing with multiple, equivalent optima.

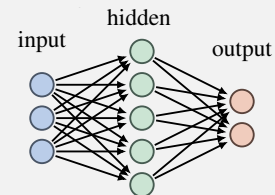
Box B: Machine learning and neural networks

The basic idea of **ML** is to train a computer to solve a specific task without explicitly instructing it how to operate. Central to this approach is the availability of large amounts of data (or the possibility to synthetically generate them). **ML** can be employed to address various tasks²⁶⁴ that can be grouped into different types. For instance, three important **ML** tasks are (i) the **classification** of data into categories, (ii) the **regression** of functions given their values on data vectors, and (iii) the **sampling** of new data vectors that are distributed similar to vectors in the given data. A central goal of **ML** algorithms is generalisability, i.e., the computer should succeed in the given task not only for the given training data, but also when new data are provided after the learning phase. This can be monitored by dividing the available data set into training and test subsets, which are used to train and test the algorithm, respectively.

The basic building block of several modern **ML** architectures is the **artificial neuron**. These are single-output nonlinear functions $n : \mathbb{R}^n \rightarrow \mathbb{R}$ typically modeled as $n(\mathbf{x}) = f(\mathbf{W} \cdot \mathbf{x} + b)$, where $f : \mathbb{R} \rightarrow \mathbb{R}$ is a fixed nonlinear (activation) function, and the weights \mathbf{W} and optional biases b are optimised during the training phase. As a single neuron is not sufficient to approximate complex dependencies, multiple neurons are arranged and connected to form a **NN**.

Widely used **NN** architectures include:

(1) **Dense feedforward NNs**, with neurons grouped into several layers, where the initial and final layer describe the input and output, respectively. Any neuron can be influenced by any other neuron of the previous layer, and can influence any neuron of the subsequent layer. The intermediate (hidden) layers generate the expressivity of the **NN**, where the number of hidden layers and the number of neurons in the hidden layers are called the depth and the width of the **NN**, respectively.



(2) Feedforward **NNs** can be equipped with **convolutional layers**, in which each neuron is influenced by only a part of the previous layer by means of a convolutional filter or kernel. This filter is the same for all neurons of a layer, significantly reducing memory and training time requirements. Convolutional layers are particularly suitable to recognise and extract regular patterns.

(3) Recurrent neural networks (**RNNs**) allow for retaining memory between the processing of subsequent inputs. This approach is often used in time-series or feedback-control scenarios.

(4) A Restricted Boltzmann Machine (**RBM**) employs a visible layer that is connected to one or several hidden layers. The (undirected) interlayer connections represent the weights of a Gibbs distribution, such that they can be efficiently trained via Gibbs sampling. **RBM**s are used to model discrete probability distributions.

(5) Generative adversarial networks (**GANs**) consist of two separate and competing **NNs**, the generator and the discriminator. The discriminator is trained to distinguish genuine data from that generated by the generator. The resulting adversarial game converges when the generator is capable of fooling the discriminator, by generating data that are indistinguishable from genuine ones.

A large enough **NN** is known to be a universal function approximator²⁶⁵. However, the size of the **NN** should be carefully chosen as its trainability can be compromised when chosen too large, and its generalisability may also suffer in presence of a high expressivity and long training schedules (overfitting). To train the **NN**, one must choose a problem-specific cost function that can be minimised via stochastic gradient descent. The way the **NN** is trained depends on the given task and is generally divided into three categories:

Supervised learning	Unsupervised learning	Reinforcement learning
The training data are labeled with their target values, i.e., the target function that should be learned by the NN is known for the training data.	The training data are not labeled and the NN is trained to recognise any type of structure or pattern in the data.	There is no training data, but the NN is connected to an environment. The NN is trained to maximise a reward that is assigned according to the NN 's actions.

Finally, we want to mention the recent introductions of neural ordinary differential equations) **NODEs** and physics-inspired neural networks (**PINNs**). **NODEs** model differential equations¹⁴⁴ (or a Lagrangian function¹⁴⁵) with a **NN**. In particular, given the current state of the system, $u(\mathbf{x}, t)$, as the input, the **NN** outputs the right hand side of the differential equation, see Fig. 3(d). On the other hand, **PINNs** are trained to directly output the solution $g(\mathbf{x}, t)$ of the differential equation given the coordinates (\mathbf{x}, t) as the input. Here, the differential equations are included in the cost function (at arbitrarily chosen points $\{(\mathbf{x}_l, t_l)\}_l$) which the **PINN** tries to minimise. Boundary conditions are imposed using additional terms in the cost function¹⁴⁸ or via stronger constraints²⁶⁶.

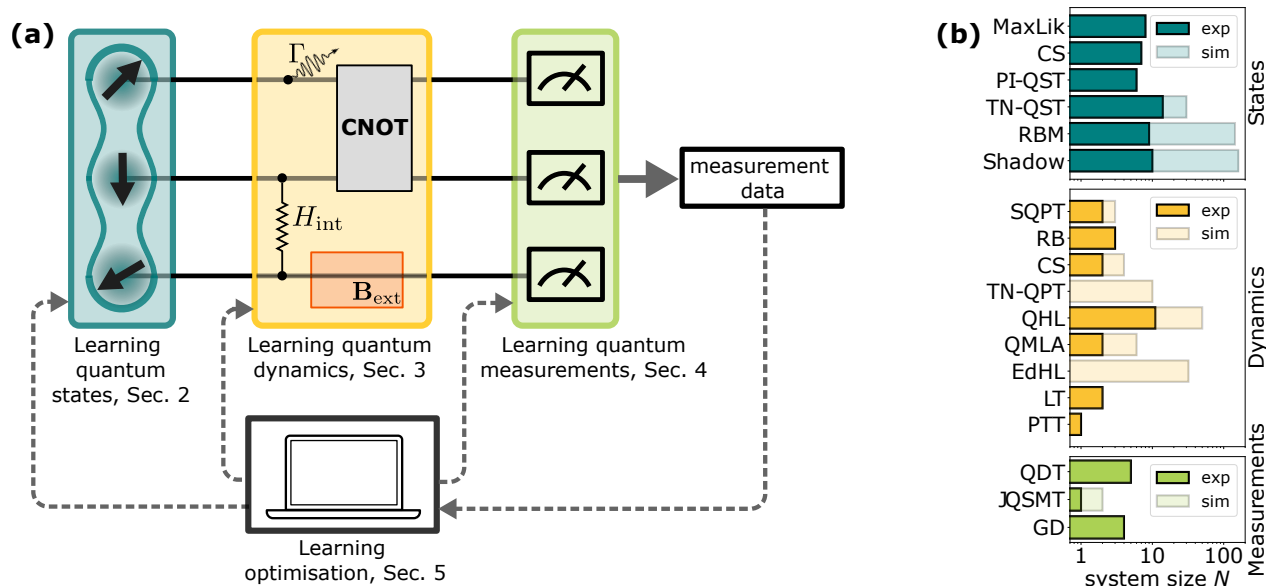


Figure 1. Learning quantum states, dynamics and measurements. (a) In this review, we divide the task of learning quantum systems into the sub-tasks of learning quantum states (Sec. 2), quantum dynamics (Sec. 3), quantum measurements (Sec. 4), and optimisation techniques (Sec. 5). (b) A list of widely-used methods for learning quantum states (top), dynamics (centre), and measurements (bottom), indicating the number of qubits N each method has been applied to for experimental and simulated data. The compared methods are (Maximum-likelihood³⁸; MaxLik), (compressed sensing⁴⁰; CS), (permutationally-invariant QST²⁶⁷; PI-QST), (tensor-network QST^{50,52}; TN-QST), (restricted Boltzmann machines^{54,58}; RBM), and (classical shadows^{66,82}; Shadow) for quantum states, (standard QPT^{102,109,114}; SQPT), (random benchmarking²⁶⁸; RB), (compressed sensing^{109,112}; CS), (tensor-network QPT¹¹⁴; TN-QPT), (quantum Hamiltonian learning^{132,134}; QHL), (quantum model learning agent¹³⁵; QMLA), (eigenstate-driven hamiltonian learning¹⁶⁷; EdHL), (Lindblad tomography¹⁷²; LT), and (process tensor tomography¹⁸¹; PTT) for quantum dynamics, and (quantum detector tomography²¹⁵; QDT), (joint quantum-state and measurement tomography^{218,219}; JQSM), and (gradient descend methods; GD) for quantum measurements.

References

1. Arute, F. et al. Quantum supremacy using a programmable superconducting processor. *Nature* **574**, 505–510, DOI: [10.1038/s41586-019-1666-5](https://doi.org/10.1038/s41586-019-1666-5) (2019).
2. Zhong, H.-S. et al. Quantum computational advantage using photons. *Science* **370**, 1460–1463, DOI: [10.1126/science.abe8770](https://doi.org/10.1126/science.abe8770) (2020). <https://www.science.org/doi/pdf/10.1126/science.abe8770>.
3. Ebadi, S. et al. Quantum phases of matter on a 256-atom programmable quantum simulator. *Nature* **595**, 227–232, DOI: [10.1038/s41586-021-03582-4](https://doi.org/10.1038/s41586-021-03582-4) (2021).
4. Feynman, R. P. Simulating physics with computers. *Int. J. Theor. Phys.* **21**, 467–488, DOI: [10.1007/BF02650179](https://doi.org/10.1007/BF02650179) (1982).
5. Preskill, J. Quantum Computing in the NISQ era and beyond. *Quantum* **2**, 79, DOI: [10.22331/q-2018-08-06-79](https://doi.org/10.22331/q-2018-08-06-79) (2018).
6. Schuld, M., Sinayskiy, I. & Petruccione, F. An introduction to quantum machine learning. *Contemp. Phys.* **56**, 172–185, DOI: [10.1080/00107514.2014.964942](https://doi.org/10.1080/00107514.2014.964942) (2015). <https://doi.org/10.1080/00107514.2014.964942>.
7. Biamonte, J. et al. Quantum machine learning. *Nature* **549**, 195–202, DOI: [10.1038/nature23474](https://doi.org/10.1038/nature23474) (2017).
8. Dunjko, V. & Briegel, H. J. Machine learning & artificial intelligence in the quantum domain: a review of recent progress. *Reports on Prog. Phys.* **81**, 074001, DOI: [10.1088/1361-6633/aab406](https://doi.org/10.1088/1361-6633/aab406) (2018).
9. Carleo, G. et al. Machine learning and the physical sciences. *Rev. Mod. Phys.* **91**, 045002, DOI: [10.1103/RevModPhys.91.045002](https://doi.org/10.1103/RevModPhys.91.045002) (2019).
10. Marquardt, F. Machine learning and quantum devices. *SciPost Phys. Lect. Notes* 029 (2021).
11. Dawid, A. et al. Modern applications of machine learning in quantum sciences. *arXiv preprint arXiv:2204.04198* (2022).
12. Bharti, K., Haug, T., Vedral, V. & Kwek, L.-C. Machine learning meets quantum foundations: A brief survey. *AVS Quantum Sci.* **2**, 034101, DOI: [10.1116/5.0007529](https://doi.org/10.1116/5.0007529) (2020).

13. Krenn, M., Erhard, M. & Zeilinger, A. Computer-inspired quantum experiments. *Nat. Rev. Phys.* **2**, 649–661, DOI: [10.1038/s42254-020-0230-4](https://doi.org/10.1038/s42254-020-0230-4) (2020).
14. Vogel, K. & Risken, H. Determination of quasiprobability distributions in terms of probability distributions for the rotated quadrature phase. *Phys. Rev. A* **40**, 2847–2849, DOI: [10.1103/PhysRevA.40.2847](https://doi.org/10.1103/PhysRevA.40.2847) (1989).
15. Raymer, M. G., Beck, M. & McAlister, D. Complex wave-field reconstruction using phase-space tomography. *Phys. Rev. Lett.* **72**, 1137–1140, DOI: [10.1103/PhysRevLett.72.1137](https://doi.org/10.1103/PhysRevLett.72.1137) (1994).
16. Leonhardt, U. Quantum-state tomography and discrete wigner function. *Phys. Rev. Lett.* **74**, 4101–4105, DOI: [10.1103/PhysRevLett.74.4101](https://doi.org/10.1103/PhysRevLett.74.4101) (1995).
17. Leibfried, D. et al. Experimental determination of the motional quantum state of a trapped atom. *Phys. Rev. Lett.* **77**, 4281–4285, DOI: [10.1103/PhysRevLett.77.4281](https://doi.org/10.1103/PhysRevLett.77.4281) (1996).
18. Hradil, Z. Quantum-state estimation. *Phys. Rev. A* **55**, R1561–R1564, DOI: [10.1103/PhysRevA.55.R1561](https://doi.org/10.1103/PhysRevA.55.R1561) (1997).
19. James, D. F. V., Kwiat, P. G., Munro, W. J. & White, A. G. Measurement of qubits. *Phys. Rev. A* **64**, 052312, DOI: [10.1103/PhysRevA.64.052312](https://doi.org/10.1103/PhysRevA.64.052312) (2001).
20. Banaszek, K., Cramer, M. & Gross, D. Focus on quantum tomography. *New J. Phys.* **15**, 125020, DOI: [10.1088/1367-2630/15/12/125020](https://doi.org/10.1088/1367-2630/15/12/125020) (2013).
21. Paris, M. G. & Rehacek, J. *Quantum state estimation*, vol. 649 (Springer, Berlin Heidelberg, 2004).
22. Lvovsky, A. I. & Raymer, M. G. Continuous-variable optical quantum-state tomography. *Rev. Mod. Phys.* **81**, 299–332, DOI: [10.1103/RevModPhys.81.299](https://doi.org/10.1103/RevModPhys.81.299) (2009).
23. Banaszek, K., D’Ariano, G. M., Paris, M. G. A. & Sacchi, M. F. Maximum-likelihood estimation of the density matrix. *Phys. Rev. A* **61**, 010304, DOI: [10.1103/PhysRevA.61.010304](https://doi.org/10.1103/PhysRevA.61.010304) (1999).
24. Smolin, J. A., Gambetta, J. M. & Smith, G. Efficient Method for Computing the Maximum-Likelihood Quantum State from Measurements with Additive Gaussian Noise. *Phys. Rev. Lett.* **108**, 070502, DOI: [10.1103/PhysRevLett.108.070502](https://doi.org/10.1103/PhysRevLett.108.070502) (2012).
25. Řeháček, J., Hradil, Z., Knill, E. & Lvovsky, A. I. Diluted maximum-likelihood algorithm for quantum tomography. *Phys. Rev. A* **75**, 042108, DOI: [10.1103/PhysRevA.75.042108](https://doi.org/10.1103/PhysRevA.75.042108) (2007).
26. Blume-Kohout, R. Optimal, reliable estimation of quantum states. *New J. Phys.* **12**, 043034, DOI: [10.1088/1367-2630/12/4/043034](https://doi.org/10.1088/1367-2630/12/4/043034) (2010).
27. Granade, C., Combes, J. & Cory, D. G. Practical Bayesian tomography. *New J. Phys.* **18**, 033024, DOI: [10.1088/1367-2630/18/3/033024](https://doi.org/10.1088/1367-2630/18/3/033024) (2016).
28. Granade, C., Ferrie, C. & Flammia, S. T. Practical adaptive quantum tomography. *New J. Phys.* **19**, 113017, DOI: [10.1088/1367-2630/aa8fe6](https://doi.org/10.1088/1367-2630/aa8fe6) (2017).
29. Granade, C. et al. QInfer: Statistical inference software for quantum applications. *Quantum* **1**, 5, DOI: [10.22331/q-2017-04-25-5](https://doi.org/10.22331/q-2017-04-25-5) (2017).
30. Christandl, M. & Renner, R. Reliable Quantum State Tomography. *Phys. Rev. Lett.* **109**, 120403, DOI: [10.1103/PhysRevLett.109.120403](https://doi.org/10.1103/PhysRevLett.109.120403) (2012).
31. Faist, P. & Renner, R. Practical and reliable error bars in quantum tomography. *Phys. Rev. Lett.* **117**, 010404, DOI: [10.1103/PhysRevLett.117.010404](https://doi.org/10.1103/PhysRevLett.117.010404) (2016).
32. Mahler, D. H. et al. Adaptive Quantum State Tomography Improves Accuracy Quadratically. *Phys. Rev. Lett.* **111**, 183601, DOI: [10.1103/PhysRevLett.111.183601](https://doi.org/10.1103/PhysRevLett.111.183601) (2013).
33. Qi, B. et al. Adaptive quantum state tomography via linear regression estimation: Theory and two-qubit experiment. *npj Quantum Inf.* **3**, 19, DOI: [10.1038/s41534-017-0016-4](https://doi.org/10.1038/s41534-017-0016-4) (2017).
34. Ferrie, C. Self-Guided Quantum Tomography. *Phys. Rev. Lett.* **113**, 190404, DOI: [10.1103/PhysRevLett.113.190404](https://doi.org/10.1103/PhysRevLett.113.190404) (2014).
35. Rambach, M. et al. Robust and efficient high-dimensional quantum state tomography. *Phys. Rev. Lett.* **126**, 100402, DOI: [10.1103/PhysRevLett.126.100402](https://doi.org/10.1103/PhysRevLett.126.100402) (2021).
36. Haah, J., Harrow, A. W., Ji, Z., Wu, X. & Yu, N. Sample-optimal tomography of quantum states. *IEEE Transactions on Inf. Theory* **63**, 5628–5641, DOI: [10.1109/TIT.2017.2719044](https://doi.org/10.1109/TIT.2017.2719044) (2017).

37. Gross, D., Liu, Y.-K., Flammia, S. T., Becker, S. & Eisert, J. Quantum State Tomography via Compressed Sensing. *Phys. Rev. Lett.* **105**, 150401, DOI: [10.1103/PhysRevLett.105.150401](https://doi.org/10.1103/PhysRevLett.105.150401) (2010).
38. Häffner, H. et al. Scalable multiparticle entanglement of trapped ions. *Nature* **438**, 643–646, DOI: [10.1038/nature04279](https://doi.org/10.1038/nature04279) (2005).
39. Flammia, S. T., Gross, D., Liu, Y.-K. & Eisert, J. Quantum tomography via compressed sensing: error bounds, sample complexity and efficient estimators. *New J. Phys.* **14**, 095022, DOI: [10.1088/1367-2630/14/9/095022](https://doi.org/10.1088/1367-2630/14/9/095022) (2012).
40. Riofrío, C. A. et al. Experimental quantum compressed sensing for a seven-qubit system. *Nat. Commun.* **8**, 15305, DOI: [10.1038/ncomms15305](https://doi.org/10.1038/ncomms15305) (2017).
41. Tóth, G. et al. Permutationally Invariant Quantum Tomography. *Phys. Rev. Lett.* **105**, 250403, DOI: [10.1103/PhysRevLett.105.250403](https://doi.org/10.1103/PhysRevLett.105.250403) (2010).
42. Moroder, T. et al. Permutationally invariant state reconstruction. *New J. Phys.* **14**, 105001, DOI: [10.1088/1367-2630/14/10/105001](https://doi.org/10.1088/1367-2630/14/10/105001) (2012).
43. Klose, G., Smith, G. & Jessen, P. S. Measuring the quantum state of a large angular momentum. *Phys. Rev. Lett.* **86**, 4721 (2001).
44. Hofmann, H. F. & Takeuchi, S. Quantum-state tomography for spin-1 systems. *Phys. Rev. A* **69**, 042108 (2004).
45. Banchi, L., Kolthammer, W. S. & Kim, M. Multiphoton tomography with linear optics and photon counting. *Phys. Rev. Lett.* **121**, 250402 (2018).
46. Titchener, J. G. et al. Scalable on-chip quantum state tomography. *npj Quantum Inf.* **4**, 1–6 (2018).
47. D’Ariano, G. M. Universal quantum observables. *Phys. Lett. A* **300**, 1–6 (2002).
48. Allahverdyan, A. E., Balian, R. & Nieuwenhuizen, T. M. Determining a quantum state by means of a single apparatus. *Phys. Rev. Lett.* **92**, 120402 (2004).
49. Perez-Garcia, D., Verstraete, F., Wolf, M. M. & Cirac, J. I. Matrix product state representations. *Quantum Info. Comput.* **7**, 401–430 (2007).
50. Cramer, M. et al. Efficient quantum state tomography. *Nat. Commun.* **1**, 149 (2010).
51. Baumgratz, T., Gross, D., Cramer, M. & Plenio, M. B. Scalable Reconstruction of Density Matrices. *Phys. Rev. Lett.* **111**, 020401, DOI: [10.1103/PhysRevLett.111.020401](https://doi.org/10.1103/PhysRevLett.111.020401) (2013).
52. Lanyon, B. P. et al. Efficient tomography of a quantum many-body system. *Nat. Phys.* **13**, 1158–1162, DOI: [10.1038/nphys4244](https://doi.org/10.1038/nphys4244) (2017).
53. Wang, J. et al. Scalable quantum tomography with fidelity estimation. *Phys. Rev. A* **101**, 032321, DOI: [10.1103/PhysRevA.101.032321](https://doi.org/10.1103/PhysRevA.101.032321) (2020).
54. Torlai, G. et al. Neural-network quantum state tomography. *Nat. Phys.* **14**, 447–450, DOI: [10.1038/s41567-018-0048-5](https://doi.org/10.1038/s41567-018-0048-5) (2018).
55. Carrasquilla, J., Torlai, G., Melko, R. G. & Aolita, L. Reconstructing quantum states with generative models. *Nat. Mach. Intell.* **1**, 155–161, DOI: [10.1038/s42256-019-0028-1](https://doi.org/10.1038/s42256-019-0028-1) (2019).
56. Morawetz, S., De Vlucht, I. J. S., Carrasquilla, J. & Melko, R. G. U(1)-symmetric recurrent neural networks for quantum state reconstruction. *Phys. Rev. A* **104**, 012401, DOI: [10.1103/PhysRevA.104.012401](https://doi.org/10.1103/PhysRevA.104.012401) (2021).
57. Palmieri, A. M. et al. Experimental neural network enhanced quantum tomography. *npj Quantum Inf.* **6**, 1–5 (2020).
58. Torlai, G. et al. Integrating Neural Networks with a Quantum Simulator for State Reconstruction. *Phys. Rev. Lett.* **123**, 230504, DOI: [10.1103/PhysRevLett.123.230504](https://doi.org/10.1103/PhysRevLett.123.230504) (2019).
59. Melkani, A., Gneiting, C. & Nori, F. Eigenstate extraction with neural-network tomography. *Phys. Rev. A* **102**, 022412, DOI: [10.1103/PhysRevA.102.022412](https://doi.org/10.1103/PhysRevA.102.022412) (2020).
60. Lloyd, S. & Weedbrook, C. Quantum generative adversarial learning. *Phys. Rev. Lett.* **121**, 040502 (2018).
61. Ahmed, S., Muñoz, C. S., Nori, F. & Kockum, A. F. Quantum state tomography with conditional generative adversarial networks. *Phys. Rev. Lett.* **127**, 140502 (2021).
62. Braccia, P., Banchi, L. & Caruso, F. Quantum noise sensing by generating fake noise. *Phys. Rev. Appl.* **17**, 024002 (2022).
63. Gühne, O. & Tóth, G. Entanglement detection. *Phys. Reports* **474**, 1–75 (2009).

64. Pezzè, L., Smerzi, A., Oberthaler, M. K., Schmied, R. & Treutlein, P. Quantum metrology with nonclassical states of atomic ensembles. *Rev. Mod. Phys.* **90**, 035005, DOI: [10.1103/RevModPhys.90.035005](https://doi.org/10.1103/RevModPhys.90.035005) (2018).
65. Brydges, T. et al. Probing Rényi entanglement entropy via randomized measurements. *Science* **364**, 260–263, DOI: [10.1126/science.aau4963](https://doi.org/10.1126/science.aau4963) (2019).
66. Elben, A. et al. Mixed-state entanglement from local randomized measurements. *Phys. Rev. Lett.* **125**, 200501, DOI: [10.1103/PhysRevLett.125.200501](https://doi.org/10.1103/PhysRevLett.125.200501) (2020).
67. Pezzè, L. & Smerzi, A. Entanglement, nonlinear dynamics, and the heisenberg limit. *Phys. Rev. Lett.* **102**, 100401, DOI: [10.1103/PhysRevLett.102.100401](https://doi.org/10.1103/PhysRevLett.102.100401) (2009).
68. Strobel, H. et al. Fisher information and entanglement of non-Gaussian spin states. *Science* **345**, 424–427, DOI: [10.1126/science.1250147](https://doi.org/10.1126/science.1250147) (2014).
69. Lu, C.-Y. et al. Experimental entanglement of six photons in graph states. *Nat. Phys.* **3**, 91–95 (2007).
70. Walborn, S., Ribeiro, P. S., Davidovich, L., Mintert, F. & Buchleitner, A. Experimental determination of entanglement with a single measurement. *Nature* **440**, 1022–1024 (2006).
71. Gray, J., Banchi, L., Bayat, A. & Bose, S. Machine-learning-assisted many-body entanglement measurement. *Phys. Rev. Lett.* **121**, 150503, DOI: [10.1103/PhysRevLett.121.150503](https://doi.org/10.1103/PhysRevLett.121.150503) (2018).
72. Gebhart, V. et al. Identifying nonclassicality from experimental data using artificial neural networks. *Phys. Rev. Res.* **3**, 023229, DOI: [10.1103/PhysRevResearch.3.023229](https://doi.org/10.1103/PhysRevResearch.3.023229) (2021).
73. Carrasquilla, J. & Melko, R. G. Machine learning phases of matter. *Nat. Phys.* **13**, 431–434, DOI: [10.1038/nphys4035](https://doi.org/10.1038/nphys4035) (2017).
74. van Nieuwenburg, E. P. L., Liu, Y.-H. & Huber, S. D. Learning phase transitions by confusion. *Nat. Phys.* **13**, 435–439, DOI: [10.1038/nphys4037](https://doi.org/10.1038/nphys4037) (2017).
75. Deng, D.-L., Li, X. & Das Sarma, S. Machine learning topological states. *Phys. Rev. B* **96**, 195145, DOI: [10.1103/PhysRevB.96.195145](https://doi.org/10.1103/PhysRevB.96.195145) (2017).
76. Rem, B. S. et al. Identifying quantum phase transitions using artificial neural networks on experimental data. *Nat. Phys.* **15**, 917–920, DOI: [10.1038/s41567-019-0554-0](https://doi.org/10.1038/s41567-019-0554-0) (2019).
77. Rodriguez-Nieva, J. F. & Scheurer, M. S. Identifying topological order through unsupervised machine learning. *Nat. Phys.* **15**, 790–795, DOI: [10.1038/s41567-019-0512-x](https://doi.org/10.1038/s41567-019-0512-x) (2019).
78. Carrasquilla, J. Machine learning for quantum matter. *Adv. Physics: X* **5**, 1797528, DOI: [10.1080/23746149.2020.1797528](https://doi.org/10.1080/23746149.2020.1797528) (2020).
79. Carrasquilla, J. & Torlai, G. How to use neural networks to investigate quantum many-body physics. *PRX Quantum* **2**, 040201, DOI: [10.1103/PRXQuantum.2.040201](https://doi.org/10.1103/PRXQuantum.2.040201) (2021).
80. Aaronson, S. The learnability of quantum states. *Proc. Royal Soc. A: Math. Phys. Eng. Sci.* **463**, 3089–3114 (2007).
81. Rocchetto, A. et al. Experimental learning of quantum states. *Sci. Adv.* **5**, 1946, DOI: [10.1126/sciadv.aau1946](https://doi.org/10.1126/sciadv.aau1946) (2019).
82. Huang, H.-Y., Kueng, R. & Preskill, J. Predicting many properties of a quantum system from very few measurements. *Nat. Phys.* **16**, 1050–1057, DOI: [10.1038/s41567-020-0932-7](https://doi.org/10.1038/s41567-020-0932-7) (2020).
83. Aaronson, S. Shadow tomography of quantum states. *SIAM J. on Comput.* **49**, 368–394, DOI: [10.1137/18M120275X](https://doi.org/10.1137/18M120275X) (2020).
84. Lukens, J. M., Law, K. J. & Bennink, R. S. A bayesian analysis of classical shadows. *npj Quantum Inf.* **7**, 1–10 (2021).
85. Huang, H.-Y., Kueng, R. & Preskill, J. Efficient estimation of pauli observables by derandomization. *Phys. Rev. Lett.* **127**, 030503, DOI: [10.1103/PhysRevLett.127.030503](https://doi.org/10.1103/PhysRevLett.127.030503) (2021).
86. Rath, A., Branciard, C., Minguzzi, A. & Vermersch, B. Quantum fisher information from randomized measurements. *Phys. Rev. Lett.* **127**, 260501, DOI: [10.1103/PhysRevLett.127.260501](https://doi.org/10.1103/PhysRevLett.127.260501) (2021).
87. Neumann, P. et al. Single-shot readout of a single nuclear spin. *Science* **329**, 542–544 (2010).
88. Myerson, A. et al. High-fidelity readout of trapped-ion qubits. *Phys. Rev. Lett.* **100**, 200502 (2008).
89. Vamivakas, A. N. et al. Observation of spin-dependent quantum jumps via quantum dot resonance fluorescence. *Nature* **467**, 297–300 (2010).
90. Elzerman, J. et al. Single-shot read-out of an individual electron spin in a quantum dot. *Nature* **430**, 431–435 (2004).

91. Magesan, E., Gambetta, J. M., Córcoles, A. D. & Chow, J. M. Machine learning for discriminating quantum measurement trajectories and improving readout. *Phys. Rev. Lett.* **114**, 200501 (2015).
92. Liu, G., Chen, M., Liu, Y.-X., Layden, D. & Cappellaro, P. Repetitive readout enhanced by machine learning. *Mach. Learn. Sci. Technol.* **1**, 015003 (2020).
93. Gambetta, J., Braff, W., Wallraff, A., Girvin, S. & Schoelkopf, R. Protocols for optimal readout of qubits using a continuous quantum nondemolition measurement. *Phys. Rev. A* **76**, 012325 (2007).
94. D’Anjou, B. & Coish, W. A. Optimal post-processing for a generic single-shot qubit readout. *Phys. Rev. A* **89**, 012313 (2014).
95. Struck, T. et al. Robust and fast post-processing of single-shot spin qubit detection events with a neural network. *Sci. Reports* **11**, 1–7 (2021).
96. Seif, A. et al. Machine learning assisted readout of trapped-ion qubits. *J. Phys. B: At. Mol. Opt. Phys.* **51**, 174006 (2018).
97. Flurin, E., Martin, L. S., Hacohen-Gourgy, S. & Siddiqi, I. Using a recurrent neural network to reconstruct quantum dynamics of a superconducting qubit from physical observations. *Phys. Rev. X* **10**, 011006 (2020).
98. Dinani, H. T., Berry, D. W., Gonzalez, R., Maze, J. R. & Bonato, C. Bayesian estimation for quantum sensing in the absence of single-shot detection. *Phys. Rev. B* **99**, 125413, DOI: [10.1103/PhysRevB.99.125413](https://doi.org/10.1103/PhysRevB.99.125413) (2019).
99. Chuang, I. L. & Nielsen, M. A. Prescription for experimental determination of the dynamics of a quantum black box. *J. Mod. Opt.* **44**, 2455–2467, DOI: [10.1080/09500349708231894](https://doi.org/10.1080/09500349708231894) (1997). <https://www.tandfonline.com/doi/pdf/10.1080/09500349708231894>.
100. Mohseni, M. & Lidar, D. A. Direct Characterization of Quantum Dynamics. *Phys. Rev. Lett.* **97**, 170501, DOI: [10.1103/PhysRevLett.97.170501](https://doi.org/10.1103/PhysRevLett.97.170501) (2006). ArXiv: quant-ph/0601033.
101. Poyatos, J. F., Cirac, J. I. & Zoller, P. Complete characterization of a quantum process: The two-bit quantum gate. *Phys. Rev. Lett.* **78**, 390–393, DOI: [10.1103/PhysRevLett.78.390](https://doi.org/10.1103/PhysRevLett.78.390) (1997).
102. Altepeter, J. B. et al. Ancilla assisted quantum process tomography. *Phys. Rev. Lett.* **90**, 193601, DOI: [10.1103/PhysRevLett.90.193601](https://doi.org/10.1103/PhysRevLett.90.193601) (2003).
103. Polino, E., Valeri, M., Spagnolo, N. & Sciarrino, F. Photonic quantum metrology. *AVS Quantum Sci.* **2**, 024703, DOI: [10.1116/5.0007577](https://doi.org/10.1116/5.0007577) (2020). <https://doi.org/10.1116/5.0007577>.
104. Mohseni, M., RezaKhani, A. T. & Lidar, D. A. Quantum-process tomography: Resource analysis of different strategies. *Phys. Rev. A* **77**, 032322, DOI: [10.1103/PhysRevA.77.032322](https://doi.org/10.1103/PhysRevA.77.032322) (2008).
105. Kosut, R., Walmsley, I. A. & Rabitz, H. Optimal experiment design for quantum state and process tomography and hamiltonian parameter estimation. *arXiv preprint quant-ph/0411093* (2004).
106. Merkel, S. T. et al. Self-consistent quantum process tomography. *Phys. Rev. A* **87**, 062119, DOI: [10.1103/PhysRevA.87.062119](https://doi.org/10.1103/PhysRevA.87.062119) (2013).
107. Knill, E. et al. Randomized benchmarking of quantum gates. *Phys. Rev. A* **77**, 012307, DOI: [10.1103/PhysRevA.77.012307](https://doi.org/10.1103/PhysRevA.77.012307) (2008).
108. Epstein, J. M., Cross, A. W., Magesan, E. & Gambetta, J. M. Investigating the limits of randomized benchmarking protocols. *Phys. Rev. A* **89**, 062321, DOI: [10.1103/PhysRevA.89.062321](https://doi.org/10.1103/PhysRevA.89.062321) (2014).
109. Rodionov, A. V. et al. Compressed sensing quantum process tomography for superconducting quantum gates. *Phys. Rev. B* **90**, 144504, DOI: [10.1103/PhysRevB.90.144504](https://doi.org/10.1103/PhysRevB.90.144504) (2014).
110. Granade, C., Ferrie, C. & Cory, D. G. Accelerated randomized benchmarking. *New J. Phys.* **17**, 013042, DOI: [10.1088/1367-2630/17/1/013042](https://doi.org/10.1088/1367-2630/17/1/013042) (2015).
111. Claes, J., Rieffel, E. & Wang, Z. Character randomized benchmarking for non-multiplicity-free groups with applications to subspace, leakage, and matchgate randomized benchmarking. *PRX Quantum* **2**, 010351, DOI: [10.1103/PRXQuantum.2.010351](https://doi.org/10.1103/PRXQuantum.2.010351) (2021).
112. Shabani, A. et al. Efficient measurement of quantum dynamics via compressive sensing. *Phys. Rev. Lett.* **106**, 100401, DOI: [10.1103/PhysRevLett.106.100401](https://doi.org/10.1103/PhysRevLett.106.100401) (2011).
113. Kosut, R. L. Quantum Process Tomography via L1-norm Minimization. *arXiv:0812.4323 [quant-ph]* (2009). ArXiv: 0812.4323.

114. Torlai, G. et al. Quantum process tomography with unsupervised learning and tensor networks. [arXiv:2006.02424 \[quant-ph\]](https://arxiv.org/abs/2006.02424) (2020). ArXiv: 2006.02424.
115. Gazit, Y., Ng, H. K. & Suzuki, J. Quantum process tomography via optimal design of experiments. *Phys. Rev. A* **100**, 012350, DOI: [10.1103/PhysRevA.100.012350](https://doi.org/10.1103/PhysRevA.100.012350) (2019).
116. Bennink, R. S. & Lougovski, P. Quantum process identification: a method for characterizing non-markovian quantum dynamics. *New J. Phys.* **21**, 083013, DOI: [10.1088/1367-2630/ab3598](https://doi.org/10.1088/1367-2630/ab3598) (2019).
117. Han, C.-D., Glaz, B., Haile, M. & Lai, Y.-C. Tomography of time-dependent quantum hamiltonians with machine learning. *Phys. Rev. A* **104**, 062404, DOI: [10.1103/PhysRevA.104.062404](https://doi.org/10.1103/PhysRevA.104.062404) (2021).
118. Carolan, J. et al. Variational quantum unsampling on a quantum photonic processor. *Nat. Phys.* **16**, 322–327, DOI: [10.1038/s41567-019-0747-6](https://doi.org/10.1038/s41567-019-0747-6) (2020).
119. Xue, S. et al. Variational quantum process tomography of unitaries. *Phys. Rev. A* **105**, 032427, DOI: [10.1103/PhysRevA.105.032427](https://doi.org/10.1103/PhysRevA.105.032427) (2022).
120. Mohseni, N., Fösel, T., Guo, L., Navarrete-Benlloch, C. & Marquardt, F. Deep Learning of Quantum Many-Body Dynamics via Random Driving. *Quantum* **6**, 714, DOI: [10.22331/q-2022-05-17-714](https://doi.org/10.22331/q-2022-05-17-714) (2022).
121. Di Franco, C., Paternostro, M. & Kim, M. S. Hamiltonian tomography in an access-limited setting without state initialization. *Phys. Rev. Lett.* **102**, 187203, DOI: [10.1103/PhysRevLett.102.187203](https://doi.org/10.1103/PhysRevLett.102.187203) (2009).
122. Cole, J. H. et al. Identifying an experimental two-state hamiltonian to arbitrary accuracy. *Phys. Rev. A* **71**, 062312, DOI: [10.1103/PhysRevA.71.062312](https://doi.org/10.1103/PhysRevA.71.062312) (2005).
123. Devitt, S. J., Cole, J. H. & Hollenberg, L. C. L. Scheme for direct measurement of a general two-qubit hamiltonian. *Phys. Rev. A* **73**, 052317, DOI: [10.1103/PhysRevA.73.052317](https://doi.org/10.1103/PhysRevA.73.052317) (2006).
124. Zhang, J. & Sarovar, M. Quantum Hamiltonian Identification from Measurement Time Traces. *Phys. Rev. Lett.* **113**, 080401, DOI: [10.1103/PhysRevLett.113.080401](https://doi.org/10.1103/PhysRevLett.113.080401) (2014).
125. Sone, A. & Cappellaro, P. Hamiltonian identifiability assisted by a single-probe measurement. *Phys. Rev. A* **95**, 022335, DOI: [10.1103/PhysRevA.95.022335](https://doi.org/10.1103/PhysRevA.95.022335) (2017).
126. Hangleiter, D., Roth, I., Eisert, J. & Roushan, P. Precise hamiltonian identification of a superconducting quantum processor. [arXiv:2108.08319](https://arxiv.org/abs/2108.08319) (2021). [2108.08319](https://arxiv.org/abs/2108.08319).
127. Evans, T. et al. Fast bayesian tomography of a two-qubit gate set in silicon. *Phys. Rev. Appl.* **17**, 024068 (2022).
128. Granade, C. E., Ferrie, C., Wiebe, N. & Cory, D. G. Robust online Hamiltonian learning. *New J. Phys.* **14**, 103013, DOI: [10.1088/1367-2630/14/10/103013](https://doi.org/10.1088/1367-2630/14/10/103013) (2012).
129. Wiebe, N., Granade, C., Ferrie, C. & Cory, D. Hamiltonian Learning and Certification Using Quantum Resources. *Phys. Rev. Lett.* **112**, 190501, DOI: [10.1103/PhysRevLett.112.190501](https://doi.org/10.1103/PhysRevLett.112.190501) (2014).
130. Wiebe, N., Granade, C., Ferrie, C. & Cory, D. Quantum Hamiltonian learning using imperfect quantum resources. *Phys. Rev. A* **89**, 042314, DOI: [10.1103/PhysRevA.89.042314](https://doi.org/10.1103/PhysRevA.89.042314) (2014).
131. Stenberg, M. P., Sanders, Y. R. & Wilhelm, F. K. Efficient Estimation of Resonant Coupling between Quantum Systems. *Phys. Rev. Lett.* **113**, 210404, DOI: [10.1103/PhysRevLett.113.210404](https://doi.org/10.1103/PhysRevLett.113.210404) (2014).
132. Wiebe, N., Granade, C. & Cory, D. G. Quantum bootstrapping via compressed quantum Hamiltonian learning. *New J. Phys.* **17**, 022005, DOI: [10.1088/1367-2630/17/2/022005](https://doi.org/10.1088/1367-2630/17/2/022005) (2015).
133. Wang, J. et al. Experimental quantum Hamiltonian learning. *Nat. Phys.* **13**, 551–555, DOI: [10.1038/nphys4074](https://doi.org/10.1038/nphys4074) (2017).
134. Hou, P.-Y. et al. Experimental hamiltonian learning of an 11-qubit solid-state quantum spin register. *Chin. Phys. Lett.* **36**, 100303 (2019).
135. Gentile, A. A. et al. Learning models of quantum systems from experiments. *Nat. Phys.* 1–7, DOI: [10.1038/s41567-021-01201-7](https://doi.org/10.1038/s41567-021-01201-7) (2021).
136. Hincks, I., Granade, C. & Cory, D. G. Statistical inference with quantum measurements: methodologies for nitrogen vacancy centers in diamond. *New J. Phys.* **20**, 013022, DOI: [10.1088/1367-2630/aa9c9f](https://doi.org/10.1088/1367-2630/aa9c9f) (2018).
137. Santagati, R. et al. Magnetic-Field Learning Using a Single Electronic Spin in Diamond with One-Photon Readout at Room Temperature. *Phys. Rev. X* **9**, 021019, DOI: [10.1103/PhysRevX.9.021019](https://doi.org/10.1103/PhysRevX.9.021019) (2019).
138. Joas, T. et al. Online adaptive quantum characterization of a nuclear spin. *npj Quantum Inf.* **7**, 1–8, DOI: [10.1038/s41534-021-00389-z](https://doi.org/10.1038/s41534-021-00389-z) (2021).

139. Wittler, N. et al. Integrated Tool Set for Control, Calibration, and Characterization of Quantum Devices Applied to Superconducting Qubits. *Phys. Rev. Appl.* **15**, 034080, DOI: [10.1103/PhysRevApplied.15.034080](https://doi.org/10.1103/PhysRevApplied.15.034080) (2021).
140. Schirmer, S. G. & Langbein, F. C. Ubiquitous problem of learning system parameters for dissipative two-level quantum systems: Fourier analysis versus bayesian estimation. *Phys. Rev. A* **91**, 022125 (2015).
141. Flynn, B., Gentile, A. A., Wiebe, N., Santagati, R. & Laing, A. Quantum model learning agent: characterisation of quantum systems through machine learning. *New J. Phys.* **24**, 053034 (2022).
142. Xin, T. et al. Local-measurement-based quantum state tomography via neural networks. *npj Quantum Inf.* **5**, 1–8, DOI: [10.1038/s41534-019-0222-3](https://doi.org/10.1038/s41534-019-0222-3) (2019).
143. Che, L. et al. Learning quantum hamiltonians from single-qubit measurements. *Phys. Rev. Res.* **3**, 023246, DOI: [10.1103/PhysRevResearch.3.023246](https://doi.org/10.1103/PhysRevResearch.3.023246) (2021).
144. Chen, R. T. Q., Rubanova, Y., Bettencourt, J. & Duvenaud, D. K. Neural ordinary differential equations. In Bengio, S. et al. (eds.) *Advances in Neural Information Processing Systems*, vol. 31 (Curran Associates, Inc., 2018).
145. Cranmer, M. et al. Lagrangian neural networks. *arXiv preprint arXiv:2003.04630* (2020).
146. Schäfer, F., Kloc, M., Bruder, C. & Lörch, N. A differentiable programming method for quantum control. *Mach. Learn. Sci. Technol.* **1**, 035009 (2020).
147. Schäfer, F., Sekatski, P., Koppenhöfer, M., Bruder, C. & Kloc, M. Control of stochastic quantum dynamics by differentiable programming. *Mach. Learn. Sci. Technol.* **2**, 035004 (2021).
148. Raissi, M., Perdikaris, P. & Karniadakis, G. E. Physics-informed neural networks: A deep learning framework for solving forward and inverse problems involving nonlinear partial differential equations. *J. Comput. Phys.* **378**, 686–707, DOI: [10.1016/j.jcp.2018.10.045](https://doi.org/10.1016/j.jcp.2018.10.045) (2019).
149. Rackauckas, C. & Nie, Q. Differentialequations. jl—a performant and feature-rich ecosystem for solving differential equations in julia. *J. Open Res. Softw.* **5** (2017).
150. Lu, L., Meng, X., Mao, Z. & Karniadakis, G. E. Deepxde: A deep learning library for solving differential equations. *SIAM Rev.* **63**, 208–228 (2021).
151. Haghighat, E. & Juanes, R. Sciann: A keras/tensorflow wrapper for scientific computations and physics-informed deep learning using artificial neural networks. *Comput. Methods Appl. Mech. Eng.* **373**, 113552 (2021).
152. Hennigh, O. et al. Nvidia simnet™: An ai-accelerated multi-physics simulation framework. In *International Conference on Computational Science*, 447–461 (Springer, 2021).
153. Both, G. J., Choudhury, S., Sens, P. & Kusters, R. DeepMoD: Deep learning for model discovery in noisy data. *J. Comput. Phys.* **428**, 109985, DOI: [10.1016/j.jcp.2020.109985](https://doi.org/10.1016/j.jcp.2020.109985) (2021). [1904.09406](https://arxiv.org/abs/1904.09406).
154. Heim, N., Ghosh, A., Kyriienko, O. & Elfving, V. E. Quantum Model-Discovery. *arXiv:2111.06376* 1–19 (2021). [2111.06376](https://arxiv.org/abs/2111.06376).
155. Benedetti, M., Lloyd, E., Sack, S. & Fiorentini, M. Parameterized quantum circuits as machine learning models. *Quantum Sci. Technol.* **4**, DOI: [10.1088/2058-9565/ab4eb5](https://doi.org/10.1088/2058-9565/ab4eb5) (2019). [1906.07682](https://arxiv.org/abs/1906.07682).
156. Goto, T., Tran, Q. H. & Nakajima, K. Universal Approximation Property of Quantum Machine Learning Models in Quantum-Enhanced Feature Spaces. *Phys. Rev. Lett.* **127**, DOI: [10.1103/PhysRevLett.127.090506](https://doi.org/10.1103/PhysRevLett.127.090506) (2021). [2009.00298](https://arxiv.org/abs/2009.00298).
157. McClean, J. R., Boixo, S., Smelyanskiy, V. N., Babbush, R. & Neven, H. Barren plateaus in quantum neural network training landscapes. *Nat. Commun.* **9**, 1–6, DOI: [10.1038/s41467-018-07090-4](https://doi.org/10.1038/s41467-018-07090-4) (2018). [1803.11173](https://arxiv.org/abs/1803.11173).
158. Kyriienko, O., Paine, A. E. & Elfving, V. E. Solving nonlinear differential equations with differentiable quantum circuits. *Phys. Rev. A* **103**, 1–22, DOI: [10.1103/PhysRevA.103.052416](https://doi.org/10.1103/PhysRevA.103.052416) (2021). [2011.10395](https://arxiv.org/abs/2011.10395).
159. Elhamod, M. et al. Learning physics-guided neural networks with competing physics loss: A summary of results in solving eigenvalue problems. In *AAAI Spring Symposium: MLPS* (2021).
160. Güngördü, U. & Kestner, J. P. Robust quantum gates using smooth pulses and physics-informed neural networks. *Phys. Rev. Res.* **4**, 023155, DOI: [10.1103/PhysRevResearch.4.023155](https://doi.org/10.1103/PhysRevResearch.4.023155) (2022).
161. Youssry, A., Chapman, R. J., Peruzzo, A., Ferrie, C. & Tomamichel, M. Modeling and control of a reconfigurable photonic circuit using deep learning. *Quantum Sci. Technol.* **5**, 025001, DOI: [10.1088/2058-9565/ab60de](https://doi.org/10.1088/2058-9565/ab60de) (2020).
162. Youssry, A. et al. Experimental graybox quantum control, DOI: [10.48550/ARXIV.2206.12201](https://doi.org/10.48550/ARXIV.2206.12201) (2022).

163. Qi, X.-L. & Ranard, D. Determining a local Hamiltonian from a single eigenstate. *Quantum* **3**, 159, DOI: [10.22331/q-2019-07-08-159](https://doi.org/10.22331/q-2019-07-08-159) (2019).
164. Chertkov, E. & Clark, B. K. Computational inverse method for constructing spaces of quantum models from wave functions. *Phys. Rev. X* **8**, 031029 (2018).
165. Greiter, M., Schnells, V. & Thomale, R. Method to identify parent hamiltonians for trial states. *Phys. Rev. B* **98**, 081113 (2018).
166. Bairey, E., Arad, I. & Lindner, N. H. Learning a Local Hamiltonian from Local Measurements. *Phys. Rev. Lett.* **122**, 020504, DOI: [10.1103/PhysRevLett.122.020504](https://doi.org/10.1103/PhysRevLett.122.020504) (2019).
167. Zhu, W., Huang, Z. & He, Y.-C. Reconstructing entanglement hamiltonian via entanglement eigenstates. *Phys. Rev. B* **99**, 235109 (2019).
168. Breuer, H., Petruccione, F. & Petruccione, S. *The Theory of Open Quantum Systems* (Oxford University Press, 2002).
169. Leggett, A. J. et al. Dynamics of the dissipative two-state system. *Rev. Mod. Phys.* **59**, 1–85, DOI: [10.1103/RevModPhys.59.1](https://doi.org/10.1103/RevModPhys.59.1) (1987).
170. Gorini, V., Kossakowski, A. & Sudarshan, E. C. G. Completely positive dynamical semigroups of n-level systems. *J. Math. Phys.* **17**, 821–825 (1976).
171. Lindblad, G. On the generators of quantum dynamical semigroups. *Commun. Math. Phys.* **48**, 119–130 (1976).
172. Samach, G. O. et al. Lindblad tomography of a superconducting quantum processor. *arXiv preprint arXiv:2105.02338* (2021).
173. Zhang, J. & Sarovar, M. Identification of open quantum systems from observable time traces. *Phys. Rev. A* **91**, 052121, DOI: [10.1103/PhysRevA.91.052121](https://doi.org/10.1103/PhysRevA.91.052121) (2015).
174. Bairey, E., Guo, C., Poletti, D., Lindner, N. H. & Arad, I. Learning the dynamics of open quantum systems from their steady states. *New J. Phys.* **22**, 032001 (2020).
175. Rivas, Á. & Huelga, S. *Open Quantum Systems: An Introduction*. SpringerBriefs in Physics (Springer Berlin Heidelberg, 2011).
176. Li, L., Hall, M. J. & Wiseman, H. M. Concepts of quantum non-markovianity: A hierarchy. *Phys. Reports* **759**, 1–51 (2018).
177. Pollock, F. A., Rodríguez-Rosario, C., Frauenheim, T., Paternostro, M. & Modi, K. Non-markovian quantum processes: Complete framework and efficient characterization. *Phys. Rev. A* **97**, 012127 (2018).
178. Jørgensen, M. R. & Pollock, F. A. Exploiting the causal tensor network structure of quantum processes to efficiently simulate non-markovian path integrals. *Phys. Rev. Lett.* **123**, 240602, DOI: [10.1103/PhysRevLett.123.240602](https://doi.org/10.1103/PhysRevLett.123.240602) (2019).
179. Cygorek, M. et al. Simulation of open quantum systems by automated compression of arbitrary environments. *Nat. Phys.* (2022).
180. Luchnikov, I., Vintskevich, S., Grigoriev, D. & Filippov, S. Machine Learning Non-Markovian Quantum Dynamics. *Phys. Rev. Lett.* **124**, 140502, DOI: [10.1103/PhysRevLett.124.140502](https://doi.org/10.1103/PhysRevLett.124.140502) (2020).
181. White, G. A. L., Pollock, F. A., Hollenberg, L. C. L., Modi, K. & Hill, C. D. Non-markovian quantum process tomography. *PRX Quantum* DOI: [10.48550/ARXIV.2106.11722](https://doi.org/10.48550/ARXIV.2106.11722) (2022).
182. Banchi, L., Grant, E., Rocchetto, A. & Severini, S. Modelling non-markovian quantum processes with recurrent neural networks. *New J. Phys.* **20**, 123030 (2018).
183. Krastanov, S. et al. Unboxing Quantum Black Box Models: Learning Non-Markovian Dynamics. *arXiv:2009.03902* (2020).
184. Degen, C. L., Reinhard, F. & Cappellaro, P. Quantum sensing. *Rev. Mod. Phys.* **89**, 035002, DOI: [10.1103/RevModPhys.89.035002](https://doi.org/10.1103/RevModPhys.89.035002) (2017).
185. Giovannetti, V., Lloyd, S. & Maccone, L. Advances in quantum metrology. *Nat. Photonics* **5**, 222–229, DOI: [10.1038/nphoton.2011.35](https://doi.org/10.1038/nphoton.2011.35) (2011).
186. Helstrom, C. W. (ed.) *Quantum detection and estimation theory* (Academic Press, 1976).
187. Braunstein, S. L. & Caves, C. M. Statistical distance and the geometry of quantum states. *Phys. Rev. Lett.* **72**, 3439–3443, DOI: [10.1103/PhysRevLett.72.3439](https://doi.org/10.1103/PhysRevLett.72.3439) (1994).

188. Li, Y. et al. Frequentist and bayesian quantum phase estimation. *Entropy* **20**, DOI: [10.3390/e20090628](https://doi.org/10.3390/e20090628) (2018).
189. Cimini, V. et al. Calibration of Quantum Sensors by Neural Networks. *Phys. Rev. Lett.* **123**, 230502, DOI: [10.1103/PhysRevLett.123.230502](https://doi.org/10.1103/PhysRevLett.123.230502) (2019).
190. Cimini, V. et al. Calibration of Multiparameter Sensors via Machine Learning at the Single-Photon Level. *Phys. Rev. Appl.* **15**, 044003, DOI: [10.1103/PhysRevApplied.15.044003](https://doi.org/10.1103/PhysRevApplied.15.044003) (2021).
191. Nolan, S. P., Pezzè, L. & Smerzi, A. Frequentist parameter estimation with supervised learning. *AVS Quantum Sci.* **3**, 034401, DOI: [10.1116/5.0058163](https://doi.org/10.1116/5.0058163) (2021). <https://doi.org/10.1116/5.0058163>.
192. Nolan, S., Smerzi, A. & Pezzè, L. A machine learning approach to bayesian parameter estimation. *npj Quantum Inf.* **7**, 169, DOI: [10.1038/s41534-021-00497-w](https://doi.org/10.1038/s41534-021-00497-w) (2021).
193. Tóth, G. & Apellaniz, I. Quantum metrology from a quantum information science perspective. *J. Phys. A: Math. Theor.* **47**, 424006, DOI: [10.1088/1751-8113/47/42/424006](https://doi.org/10.1088/1751-8113/47/42/424006) (2014).
194. Hyllus, P. et al. Fisher information and multiparticle entanglement. *Phys. Rev. A* **85**, 022321, DOI: [10.1103/PhysRevA.85.022321](https://doi.org/10.1103/PhysRevA.85.022321) (2012).
195. Tóth, G. Multipartite entanglement and high-precision metrology. *Phys. Rev. A* **85**, 022322, DOI: [10.1103/PhysRevA.85.022322](https://doi.org/10.1103/PhysRevA.85.022322) (2012).
196. Albarelli, F., Barbieri, M., Genoni, M. & Gianani, I. A perspective on multiparameter quantum metrology: From theoretical tools to applications in quantum imaging. *Phys. Lett. A* **384**, 126311, DOI: <https://doi.org/10.1016/j.physleta.2020.126311> (2020).
197. Demkowicz-Dobrzański, R., Górecki, W. & Guţă, M. Multi-parameter estimation beyond quantum fisher information. *J. Phys. A: Math. Theor.* **53**, 363001, DOI: [10.1088/1751-8121/ab8ef3](https://doi.org/10.1088/1751-8121/ab8ef3) (2020).
198. Gessner, M., Pezzè, L. & Smerzi, A. Sensitivity bounds for multiparameter quantum metrology. *Phys. Rev. Lett.* **121**, 130503, DOI: [10.1103/PhysRevLett.121.130503](https://doi.org/10.1103/PhysRevLett.121.130503) (2018).
199. Liu, L.-Z. et al. Distributed quantum phase estimation with entangled photons. *Nat. Photonics* **15**, 137–142, DOI: [10.1038/s41566-020-00718-2](https://doi.org/10.1038/s41566-020-00718-2) (2021).
200. Moreau, P.-A., Toninelli, E., Gregory, T. & Padgett, M. J. Imaging with quantum states of light. *Nat. Rev. Phys.* **1**, 367–380 (2019).
201. Pirandola, S. On quantum reading, quantum illumination, and other notions. *IOP SciNotes* **2**, 015203 (2021).
202. Zhuang, Q. & Zhang, Z. Physical-layer supervised learning assisted by an entangled sensor network. *Phys. Rev. X* **9**, 041023 (2019).
203. Banchi, L., Zhuang, Q. & Pirandola, S. Quantum-enhanced barcode decoding and pattern recognition. *Phys. Rev. Appl.* **14**, 064026 (2020).
204. Li, Z.-M. et al. Fast correlated-photon imaging enhanced by deep learning. *Optica* **8**, 323–328 (2021).
205. Picard, L. R., Mark, M. J., Ferlaino, F. & van Bijnen, R. Deep learning-assisted classification of site-resolved quantum gas microscope images. *Meas. Sci. Technol.* **31**, 025201 (2019).
206. Harney, C., Banchi, L. & Pirandola, S. Ultimate limits of thermal pattern recognition. *Phys. Rev. A* **103**, 052406 (2021).
207. Luis, A. & Sánchez-Soto, L. L. Complete characterization of arbitrary quantum measurement processes. *Phys. Rev. Lett.* **83**, 3573–3576, DOI: [10.1103/PhysRevLett.83.3573](https://doi.org/10.1103/PhysRevLett.83.3573) (1999).
208. Fiurášek, J. Maximum-likelihood estimation of quantum measurement. *Phys. Rev. A* **64**, 024102, DOI: [10.1103/PhysRevA.64.024102](https://doi.org/10.1103/PhysRevA.64.024102) (2001).
209. D’Ariano, G. M., Maccone, L. & Presti, P. L. Quantum calibration of measurement instrumentation. *Phys. Rev. Lett.* **93**, 250407, DOI: [10.1103/PhysRevLett.93.250407](https://doi.org/10.1103/PhysRevLett.93.250407) (2004).
210. Lundeen, J. et al. Tomography of quantum detectors. *Nat. Phys.* **5**, 27–30, DOI: <https://doi.org/10.1038/nphys1133> (2009).
211. D’Auria, V., Lee, N., Amri, T., Fabre, C. & Laurat, J. Quantum decoherence of single-photon counters. *Phys. Rev. Lett.* **107**, 050504, DOI: [10.1103/PhysRevLett.107.050504](https://doi.org/10.1103/PhysRevLett.107.050504) (2011).
212. Brida, G. et al. Quantum characterization of superconducting photon counters. *New J. Phys.* **14**, 085001, DOI: [10.1088/1367-2630/14/8/085001](https://doi.org/10.1088/1367-2630/14/8/085001) (2012).

213. Zhang, L. et al. Mapping coherence in measurement via full quantum tomography of a hybrid optical detector. *Nat. Photonics* **6**, 364–368, DOI: [10.1038/nphoton.2012.107](https://doi.org/10.1038/nphoton.2012.107) (2012).
214. Grandi, S., Zavatta, A., Bellini, M. & Paris, M. G. Experimental quantum tomography of a homodyne detector. *New J. Phys.* **19**, 053015, DOI: [10.1088/1367-2630/aa6f2c](https://doi.org/10.1088/1367-2630/aa6f2c) (2017).
215. Chen, Y., Farahzad, M., Yoo, S. & Wei, T.-C. Detector tomography on ibm quantum computers and mitigation of an imperfect measurement. *Phys. Rev. A* **100**, 052315, DOI: [10.1103/PhysRevA.100.052315](https://doi.org/10.1103/PhysRevA.100.052315) (2019).
216. Renema, J. J. et al. Experimental test of theories of the detection mechanism in a nanowire superconducting single photon detector. *Phys. Rev. Lett.* **112**, 117604, DOI: [10.1103/PhysRevLett.112.117604](https://doi.org/10.1103/PhysRevLett.112.117604) (2014).
217. Mogilevtsev, D., Řeháček, J. & Hradil, Z. Self-calibration for self-consistent tomography. *New J. Phys.* **14**, 095001, DOI: [10.1088/1367-2630/14/9/095001](https://doi.org/10.1088/1367-2630/14/9/095001) (2012).
218. Keith, A. C., Baldwin, C. H., Glancy, S. & Knill, E. Joint quantum-state and measurement tomography with incomplete measurements. *Phys. Rev. A* **98**, 042318, DOI: [10.1103/PhysRevA.98.042318](https://doi.org/10.1103/PhysRevA.98.042318) (2018).
219. Zhang, A. et al. Experimental self-characterization of quantum measurements. *Phys. Rev. Lett.* **124**, 040402, DOI: [10.1103/PhysRevLett.124.040402](https://doi.org/10.1103/PhysRevLett.124.040402) (2020).
220. Higgins, B. L., Berry, D. W., Bartlett, S. D., Wiseman, H. M. & Pryde, G. J. Entanglement-free heisenberg-limited phase estimation. *Nature* **450**, 393–396, DOI: [10.1038/nature06257](https://doi.org/10.1038/nature06257) (2007).
221. Fiderer, L. J., Schuff, J. & Braun, D. Neural-network heuristics for adaptive bayesian quantum estimation. *PRX Quantum* **2**, 020303, DOI: [10.1103/PRXQuantum.2.020303](https://doi.org/10.1103/PRXQuantum.2.020303) (2021).
222. Berry, D. W. & Wiseman, H. M. Optimal states and almost optimal adaptive measurements for quantum interferometry. *Phys. Rev. Lett.* **85**, 5098–5101, DOI: [10.1103/PhysRevLett.85.5098](https://doi.org/10.1103/PhysRevLett.85.5098) (2000).
223. Hentschel, A. & Sanders, B. C. Efficient Algorithm for Optimizing Adaptive Quantum Metrology Processes. *Phys. Rev. Lett.* **107**, 233601, DOI: [10.1103/PhysRevLett.107.233601](https://doi.org/10.1103/PhysRevLett.107.233601) (2011).
224. Lovett, N. B., Crosnier, C., Perarnau-Llobet, M. & Sanders, B. C. Differential Evolution for Many-Particle Adaptive Quantum Metrology. *Phys. Rev. Lett.* **110**, 220501, DOI: [10.1103/PhysRevLett.110.220501](https://doi.org/10.1103/PhysRevLett.110.220501) (2013).
225. Pezzè, L. & Smerzi, A. Heisenberg-limited noisy atomic clock using a hybrid coherent and squeezed state protocol. *Phys. Rev. Lett.* **125**, 210503, DOI: [10.1103/PhysRevLett.125.210503](https://doi.org/10.1103/PhysRevLett.125.210503) (2020).
226. Pezzè, L. & Smerzi, A. Quantum phase estimation algorithm with gaussian spin states. *PRX Quantum* **2**, 040301, DOI: [10.1103/PRXQuantum.2.040301](https://doi.org/10.1103/PRXQuantum.2.040301) (2021).
227. Kaubruegger, R. et al. Variational spin-squeezing algorithms on programmable quantum sensors. *Phys. Rev. Lett.* **123**, 260505, DOI: [10.1103/PhysRevLett.123.260505](https://doi.org/10.1103/PhysRevLett.123.260505) (2019).
228. Kaubruegger, R., Vasilyev, D. V., Schulte, M., Hammerer, K. & Zoller, P. Quantum variational optimization of ramsey interferometry and atomic clocks. *Phys. Rev. X* **11**, 041045, DOI: [10.1103/PhysRevX.11.041045](https://doi.org/10.1103/PhysRevX.11.041045) (2021).
229. Haine, S. A. & Hope, J. J. Machine-designed sensor to make optimal use of entanglement-generating dynamics for quantum sensing. *Phys. Rev. Lett.* **124**, 060402, DOI: [10.1103/PhysRevLett.124.060402](https://doi.org/10.1103/PhysRevLett.124.060402) (2020).
230. Pang, S. & Jordan, A. N. Optimal adaptive control for quantum metrology with time-dependent Hamiltonians. *Nat. Commun.* **8**, 14695, DOI: [10.1038/ncomms14695](https://doi.org/10.1038/ncomms14695) (2017).
231. Xu, H. et al. Generalizable control for quantum parameter estimation through reinforcement learning. *npj Quantum Inf.* **5**, 1–8 (2019).
232. Bonato, C. et al. Optimized quantum sensing with a single electron spin using real-time adaptive measurements. *Nat. Nanotechnol.* **11**, 247–252, DOI: [10.1038/nnano.2015.261](https://doi.org/10.1038/nnano.2015.261) (2016).
233. Dushenko, S., Ambal, K. & McMichael, R. D. Sequential bayesian experiment design for optically detected magnetic resonance of nitrogen-vacancy centers. *Phys. Rev. Appl.* **14**, 054036, DOI: [10.1103/PhysRevApplied.14.054036](https://doi.org/10.1103/PhysRevApplied.14.054036) (2020).
234. McMichael, R. D., Dushenko, S. & Blakley, S. M. Sequential Bayesian experiment design for adaptive Ramsey sequence measurements. *J. Appl. Phys.* **130**, 144401, DOI: [10.1063/5.0055630](https://doi.org/10.1063/5.0055630) (2021).
235. Caouette-Mansour, M. et al. Robust spin relaxometry with fast adaptive bayesian estimation. *Phys. Rev. Appl.* **17**, 064031, DOI: [10.1103/PhysRevApplied.17.064031](https://doi.org/10.1103/PhysRevApplied.17.064031) (2022).
236. Bonato, C. & Berry, D. W. Adaptive tracking of a time-varying field with a quantum sensor. *Phys. Rev. A* **95**, 052348 (2017).

237. Shulman, M. D. et al. Suppressing qubit dephasing using real-time Hamiltonian estimation. *Nat. Commun.* **5**, 5156, DOI: [10.1038/ncomms6156](https://doi.org/10.1038/ncomms6156) (2014).
238. Mavadia, S., Frey, V., Sastrawan, J., Dona, S. & Biercuk, M. J. Prediction and real-time compensation of qubit decoherence via machine learning. *Nat. Commun.* **8**, 14106, DOI: [10.1038/ncomms14106](https://doi.org/10.1038/ncomms14106) (2017).
239. Cappellaro, P. Spin-bath narrowing with adaptive parameter estimation. *Phys. Rev. A* **85**, 030301, DOI: [10.1103/PhysRevA.85.030301](https://doi.org/10.1103/PhysRevA.85.030301) (2012).
240. Blok, M. S. et al. Manipulating a qubit through the backaction of sequential partial measurements and real-time feedback. *Nat. Phys.* **10**, 189–193, DOI: [10.1038/nphys2881](https://doi.org/10.1038/nphys2881) (2014).
241. Scerri, E., Gauger, E. M. & Bonato, C. Extending qubit coherence by adaptive quantum environment learning. *New J. Phys.* **22**, 035002, DOI: [10.1088/1367-2630/ab7bf3](https://doi.org/10.1088/1367-2630/ab7bf3) (2020).
242. Nielsen, M. A. & Chuang, I. L. *Quantum Computation and Quantum Information: 10th Anniversary Edition* (Cambridge University Press, New York, NY, USA, 2011), 10th edn.
243. Kessler, E. M., Lovchinsky, I., Sushkov, A. O. & Lukin, M. D. Quantum error correction for metrology. *Phys. Rev. Lett.* **112**, 150802, DOI: [10.1103/PhysRevLett.112.150802](https://doi.org/10.1103/PhysRevLett.112.150802) (2014).
244. Arrad, G., Vinkler, Y., Aharonov, D. & Retzker, A. Increasing sensing resolution with error correction. *Phys. Rev. Lett.* **112**, 150801, DOI: [10.1103/PhysRevLett.112.150801](https://doi.org/10.1103/PhysRevLett.112.150801) (2014).
245. Dür, W., Skotiniotis, M., Fröwis, F. & Kraus, B. Improved quantum metrology using quantum error correction. *Phys. Rev. Lett.* **112**, 080801, DOI: [10.1103/PhysRevLett.112.080801](https://doi.org/10.1103/PhysRevLett.112.080801) (2014).
246. Zhou, S., Zhang, M., Preskill, J. & Jiang, L. Achieving the heisenberg limit in quantum metrology using quantum error correction. *Nat. Commun.* **9**, 78, DOI: [10.1038/s41467-017-02510-3](https://doi.org/10.1038/s41467-017-02510-3) (2018).
247. Górecki, W., Zhou, S., Jiang, L. & Demkowicz-Dobrzański, R. Optimal probes and error-correction schemes in multi-parameter quantum metrology. *Quantum* **4**, 288, DOI: [10.22331/q-2020-07-02-288](https://doi.org/10.22331/q-2020-07-02-288) (2020).
248. Innocenti, L., Banchi, L., Ferraro, A., Bose, S. & Paternostro, M. Supervised learning of time-independent hamiltonians for gate design. *New J. Phys.* **22**, 065001, DOI: [10.1088/1367-2630/ab8aaf](https://doi.org/10.1088/1367-2630/ab8aaf) (2020).
249. Gao, X., Erhard, M., Zeilinger, A. & Krenn, M. Computer-inspired concept for high-dimensional multipartite quantum gates. *Phys. Rev. Lett.* **125**, 050501, DOI: [10.1103/PhysRevLett.125.050501](https://doi.org/10.1103/PhysRevLett.125.050501) (2020).
250. Valenti, A., van Nieuwenburg, E., Huber, S. & Greplova, E. Hamiltonian learning for quantum error correction. *Phys. Rev. Res.* **1**, 033092, DOI: [10.1103/PhysRevResearch.1.033092](https://doi.org/10.1103/PhysRevResearch.1.033092) (2019).
251. Fösel, T., Tighineanu, P., Weiss, T. & Marquardt, F. Reinforcement learning with neural networks for quantum feedback. *Phys. Rev. X* **8**, 031084, DOI: [10.1103/PhysRevX.8.031084](https://doi.org/10.1103/PhysRevX.8.031084) (2018).
252. Bukov, M. et al. Reinforcement learning in different phases of quantum control. *Phys. Rev. X* **8**, 031086 (2018).
253. Niu, M. Y., Boixo, S., Smelyanskiy, V. N. & Neven, H. Universal quantum control through deep reinforcement learning. *npj Quantum Inf.* **5**, 1–8 (2019).
254. Baum, Y. et al. Experimental deep reinforcement learning for error-robust gate-set design on a superconducting quantum computer. *PRX Quantum* **2**, 040324 (2021).
255. Nguyen, V. et al. Deep reinforcement learning for efficient measurement of quantum devices. *npj Quantum Inf.* **7**, 1–9 (2021).
256. Sivak, V. et al. Model-free quantum control with reinforcement learning. *Phys. Rev. X* **12**, 011059 (2022).
257. Kottmann, J. S., Krenn, M., Kyaw, T. H., Alperin-Lea, S. & Aspuru-Guzik, A. Quantum computer-aided design of quantum optics hardware. *Quantum Sci. Technol.* **6**, 035010, DOI: [10.1088/2058-9565/abfc94](https://doi.org/10.1088/2058-9565/abfc94) (2021).
258. Huang, H.-Y. et al. Quantum advantage in learning from experiments. *Science* **376**, 1182–1186, DOI: [10.1126/science.abn7293](https://doi.org/10.1126/science.abn7293) (2022). <https://www.science.org/doi/pdf/10.1126/science.abn7293>.
259. Wiebe, N. & Granade, C. Efficient bayesian phase estimation. *Phys. review letters* **117**, 010503 (2016).
260. Gebhart, V., Smerzi, A. & Pezzè, L. Bayesian quantum multiphase estimation algorithm. *Phys. Rev. Appl.* **16**, 014035, DOI: [10.1103/PhysRevApplied.16.014035](https://doi.org/10.1103/PhysRevApplied.16.014035) (2021).
261. Loredo, T. J. Bayesian adaptive exploration. In *AIP Conference Proceedings*, vol. 707, 330–346 (American Institute of Physics, 2004).

262. Del Moral, P., Doucet, A. & Jasra, A. Sequential monte carlo samplers. *J. Royal Stat. Soc. Ser. B (Statistical Methodol.* **68**, 411–436 (2006).
263. Granade, C. & Wiebe, N. Structured filtering. *New J. Phys.* **19**, 1–22, DOI: [10.1088/1367-2630/aa77cf](https://doi.org/10.1088/1367-2630/aa77cf) (2017). [1612.00762](https://arxiv.org/abs/1612.00762).
264. Goodfellow, I., Bengio, Y. & Courville, A. *Deep learning* (MIT press, 2016).
265. Hornik, K. Some new results on neural network approximation. *Neural Networks* **6**, 1069–1072, DOI: [10.1016/S0893-6080\(09\)80018-X](https://doi.org/10.1016/S0893-6080(09)80018-X) (1993).
266. Moseley, B., Markham, A. & Nissen-Meyer, T. Finite Basis Physics-Informed Neural Networks (FBPINNs): a scalable domain decomposition approach for solving differential equations. *arXiv:2107.07871* (2021). [2107.07871](https://arxiv.org/abs/2107.07871).
267. Schwemmer, C. et al. Experimental Comparison of Efficient Tomography Schemes for a Six-Qubit State. *Phys. Rev. Lett.* **113**, 040503, DOI: [10.1103/PhysRevLett.113.040503](https://doi.org/10.1103/PhysRevLett.113.040503) (2014).
268. McKay, D. C., Sheldon, S., Smolin, J. A., Chow, J. M. & Gambetta, J. M. Three-qubit randomized benchmarking. *Phys. Rev. Lett.* **122**, 200502, DOI: [10.1103/PhysRevLett.122.200502](https://doi.org/10.1103/PhysRevLett.122.200502) (2019).
269. Lennon, D. T. et al. Efficiently measuring a quantum device using machine learning. *npj Quantum Inf.* **5**, 1–8 (2019).
270. Porotti, R., Essig, A., Huard, B. & Marquardt, F. Deep Reinforcement Learning for Quantum State Preparation with Weak Nonlinear Measurements. *Quantum* **6**, 747, DOI: [10.22331/q-2022-06-28-747](https://doi.org/10.22331/q-2022-06-28-747) (2022).

Acronyms

GAN Generative Adversarial Network.

GKS-L Gorini, Kossakowski, Sudarshan and Lindblad.

ML Machine Learning.

NN Neural Network.

NODE Neural Ordinary Differential Equation.

PINN Physics-Informed Neural Network.

POVM Positive-Operator Valued Measure.

QDT Quantum Detection Tomography.

QFI Quantum Fisher Information.

QHL Quantum Hamiltonian Learning.

QMLA Quantum Model Learning Agent.

QPT Quantum Process Tomography.

QST Quantum State Tomography.

RBM Restricted Boltzmann Machine.

RL Reinforcement Learning.

RNN Recurrent Neural Network.

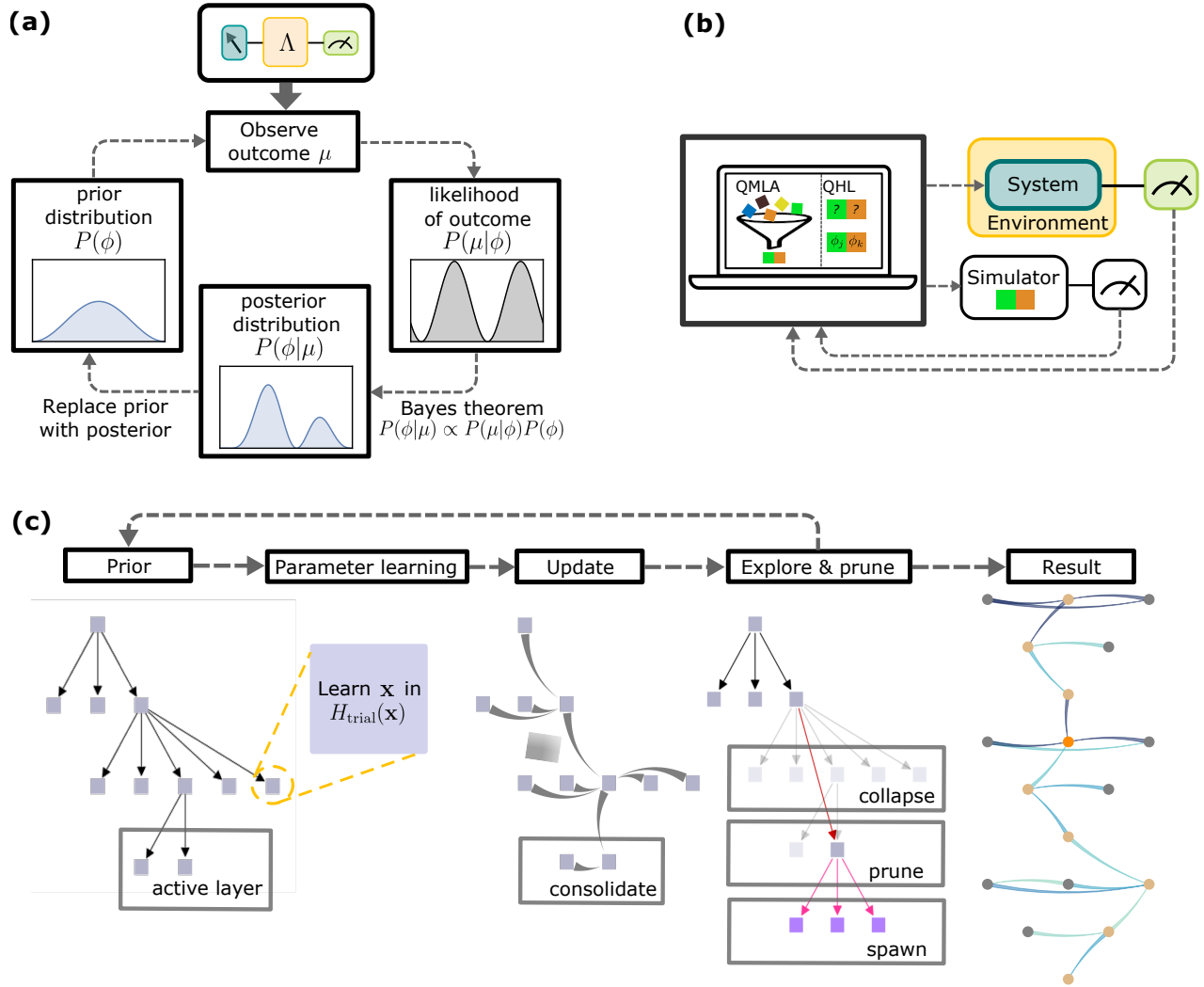


Figure 2. Bayesian inference for parameter estimation and model learning. (a) Bayesian inference enables to learn the probability distribution for unknown parameters by applying Bayes rules with the measurement outcome of each experiment performed on the quantum system (Box A). (b) An overview of the principal subtending protocols for learning quantum dynamics that employ a (quantum) simulator^{128–130,132–136,141}. For each iteration i , identical fiducial states $|\psi\rangle_{\text{trial}}$ are prepared and fed to both the system to be characterised and the simulator, where $|\psi\rangle_{\text{trial}}$ undergoes evolution for a predetermined time t . The latter is assumed to be tunable, to dial the trial Hamiltonian $H_{\text{trial}}(\mathbf{x})$, whose parametrised terms are symbolically rendered by coloured squares, which is either known (e.g. in QHL) or hypothesised (e.g. in QMLA). The outcome μ_i collected at the end of each epoch is then fed into the protocol to perform the relevant inference (see also c). (c) An outline of the protocols that have been demonstrated for model learning, QMLA^{135,141}. The information gathered from experiments is stored in a tree structure, whose leaves are candidate Hamiltonians $H_{\text{trial}}(\mathbf{x})$. The paramatisation for those Hamiltonians in the active layer is learned by a method of choice. Trained, active candidate models ($H_{\text{trial},i}, H_{\text{trial},j}$) are then pairwise compared according to a metric \mathcal{B}_{ij} , capturing the relative performance at reproducing the unknown system and stored as edges of the graph. According to the global outcomes, single nodes or entire layers can be discarded, and relevant terms spawned to new candidate Hamiltonians.

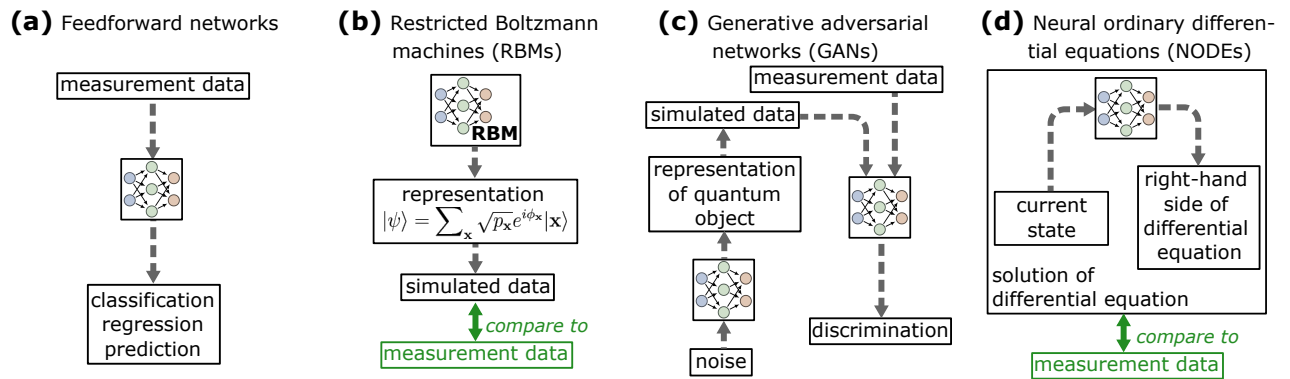
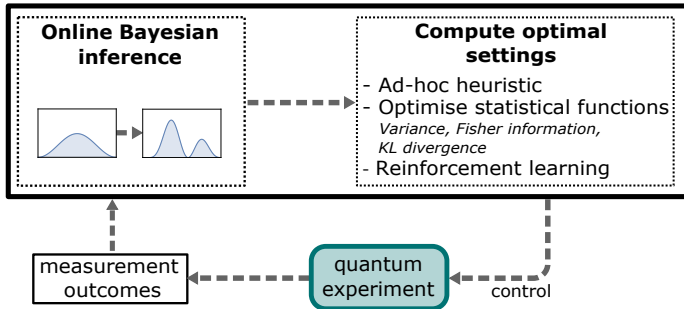
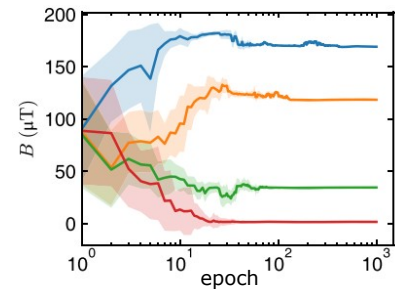


Figure 3. Different examples of neural networks for learning quantum systems. NNs have been employed after the acquisition of measurement data (i.e., in the post-processing) as (a) feedforward NNs for the classification^{71–73} and regression²⁶⁴ of measurement data, and the prediction of quantum dynamics⁹⁷, (b) as RBMs for QST^{54,55}, (c) as GANs for the tomography of quantum states⁶¹ and processes⁶², and (d) as NODEs for optimal quantum control^{146,147}. Alternatively to NODE, PINNs (that include the differential equation in the cost function) have been used for creating robust quantum gates¹⁶⁰.

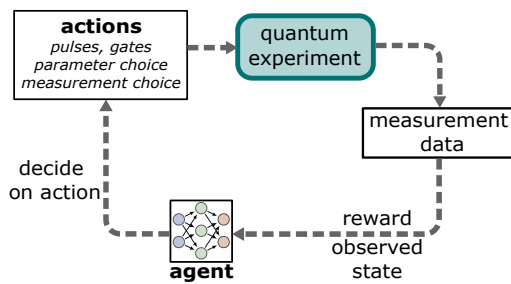
(a) Adaptive Bayesian experiment optimisation



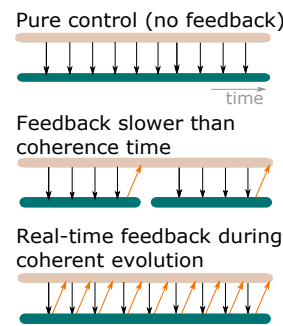
(b)



(c) Reinforcement learning on quantum experiment



(d) Types of control



(e)

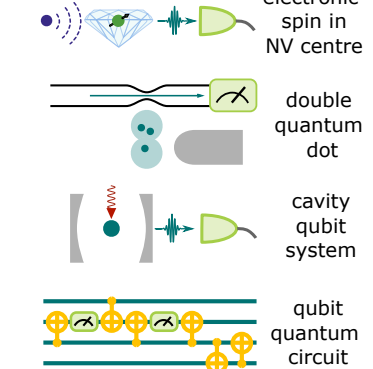


Figure 4. Optimising quantum experiments (a) Example of adaptive experimental control, through Bayesian inference. After each measurement, the outcome is used to update the current probability distribution for the parameters of interest. This probability distribution is then used to compute optimal settings for the next measurement, through ad-hoc heuristics, the optimisation of statistical quantities (variance, Fisher information, Kullback-Leibler divergence, etc) (b) Adaptive Bayesian optimisation has been used, for example, to optimise magnetic sensing using the single electronic spin associated to an NV centre in diamond. In the plot, from T. Joas et al¹³⁸, as estimation epochs increase, the magnetic field value converges to the ground truth (solid lines) and the standard deviation (shaded areas) decrease. (c) Schematic feedback loop optimised via RL. Measurement results are fed into an agent that decides on the next action to apply to the quantum experiment. (d) Different scenarios for optimised quantum control; time evolution, with control pulses as black arrows, measurements as orange arrows, agent in brown, and the quantum experiments' coherent evolution intervals in green. (e) Adaptive Bayesian inference and RL have been applied to or suggested for several experimental quantum systems, such as NV centres^{137,138,232–235}, quantum dots^{255,269}, cavity-qubit systems^{256,270} and multi-qubit systems with gates applied as actions and subject to projective measurements²⁵¹